TRABAJO FIN DE GRADO

GRADO EN FÍSICA

Propagación de ondas en la atmósfera solar: Estudio de la transformación de modos en la frontera fotosfera-cromosfera

Autora: Ángeles Moreno Guedes

Tutores: Martín Manuel Gómez Míguez (ULL, IAC) y
David Martínez Gómez (IAC, ULL)

Curso 2022-2023

Resumen

Uno de los problemas abiertos en física solar es el calentamiento cromosférico. En la actualidad, todavía no se ha encontrado un mecanismo de transporte que llegue a explicar el alto aumento de temperatura que se observa en dicha región de la atmósfera solar. Uno de los mecanismos comúnmente propuestos es la disipación de la energía transportada por las ondas que se propagan desde las capas bajas de la atmósfera. Por otra parte, el estudio de la propagación de las ondas que se generan en el Sol es también de gran relevancia, porque permite desentrañar algunas de las propiedades físicas de su estructura y dinámica.

Este trabajo se centra en estudiar la propagación de ondas en la frontera de la fotosfera-cromosfera y el estudio de la transformación de modos. La principal motivación es la derivación de las propiedades de los modos de propagación de las ondas en estas regiones (fotosfera, cromosfera y su frontera), ya que los mecanismos de liberación de energía varían según la naturaleza de los modos, por lo que caracterizarlos físicamente es de gran importancia. De forma más precisa, en este trabajo vamos a realizar un estudio general de distintas ondas que se pueden propagar en la atmósfera solar (ondas acústicas, acústico-gravitatorias, ondas magneto-acústicas y ondas de Alfvén) para después pasar al caso concreto de la propagación de las ondas magneto-acústicas en la frontera. Estas ondas presentan dos modos característicos: el rápido y el lento. Estos últimos se caracterizan por tener una naturaleza acústica o magnética dependiendo de si se encuentran en la fotosfera, donde dominan las fuerzas hidrodinámicas del plasma o en la cromosfera, donde dominan las magnéticas. Es de esperar que en la región frontera, la región de equipartición, estas fuerzas sean comparables, lo cual afectaría a la naturaleza de los modos volviéndolos indistinguibles. Esto podría producir una transferencia de energía de un modo a otro, es decir, tendría lugar el fenómeno de transformación de modos.

En primer lugar, presentamos el modelo de las ecuaciones magnetohidrodinámicas (MHD) ideales que nos permite describir la dinámica del plasma de la atmósfera solar dentro del estudio que nos interesa. Después, entramos en una de las partes principales del trabajo, en la cual se realiza un estudio general de la propagación de ondas en la atmósfera solar por el método de pequeñas perturbaciones y linearización de las ecuaciones MHD ideales. Primero comenzamos con la caracterización del medio, una atmósfera estratificada en la dirección vertical e isoterma, por la cual nuestras ondas se propagarán. En esta primera parte, en la que linearizamos las ecuaciones MHD ideales, partiremos ignorando los efectos del campo magnético y con una configuración 1D. Esto nos permite describir las ondas acústicas en un medio estratificado. Después, se continuará con la descripción y derivación de la relación de dispersión de las ondas acústico-gravitatorias, pero ahora ya en 2D. Además, se discutirá la relevancia de frecuencias clave en la propagación de ondas en un medio estratificado, como son la frecuencia de corte y la frecuencia de Brunt-Väisälä. A continuación, incluimos el campo magnético y en 3D, pero trabajando en esta ocasión, con un medio homogéneo, ya que simplificará la complejidad algebraica. Aquí se derivarán las relaciones de dispersión de las ondas Alfvén y los dos modos de las ondas magnetoacústicas, el rápido y el lento mediante una descripción 3D. Pero después se simplificará a una en 2D, debido a que las ondas Alfvén están polarizadas en la dirección ortogonal al plano que forman el campo magnético y el vector de onda. Esto nos permitirá trabajar en dicho plano donde se encuentran las ondas del modo rápido y lento ignorando a las de Alfvén de nuestro estudio, ya que solo estamos interesados en la descripción de los modos rápido y lento. A partir de ahí, trabajaremos siempre con estos dos modos. Derivaremos que en los límites en los que predominan las fuerzas hidrodinámicas o, en el caso contrario, las magnéticas, ambos modos tienen unas propiedades bien diferenciadas asociadas a dichas condiciones del medio. En la conclusión de esta primera parte se deriva la ecuación de conservación de energía para las ondas magnetoacústicas, llegando al resultado de que bajo ciertas condiciones que se suelen cumplir, las ondas magnetoacústicas conservan la energía. Este resultado nos proporciona una condición importante que nos permite aplicar el formalismo de trazado de rayos que se describe en la siguiente parte del trabajo.

En la siguiente parte de este estudio, se aplica el método de aproximación de trazado de rayos, que permite extender los resultados obtenidos para las ondas magnetoacústicas añadiendo una estratificación en las variables del medio, como son la presión y la densidad. Dicho medio lo consideramos débilmente inhomogéneo, puesto que en nuestro caso consideramos que las escalas características de la atmósfera son mucho mayores que la longitud de onda. Es posible utilizar los términos manipulados en las ondas magnetoacústicas, ya que el trabajar a frecuencias altas (mayores que la frecuencia de corte y de Brunt Väisälä) nos permite despreciar los términos proporcionales a la escala de presiones, provocando que sean los mismos que para un medio homogéneo. El fin de aplicar dicho método es simplificar el estudio incluso extendiéndolo a un medio inhomogéneo, aunque entorno a la región de equipartición, el método de trazado de rayos falla y se hace necesario realizar una conexión en dicho punto. Este método es el que sigue Tracy et al. (2014), este formalismo nos permite ver que en esta región los modos de las ondas magnetoacústicas se vuelven indistinguibles debido a que la fuerzas hidrodinámicas y magnéticas son comparables. A partir de esto último llegamos a nuestro resultado más importante: en la región cercana a la de equipartición se produce una transformación de modos. De forma más precisa esto ocurre cuando las velocidades del sonido y Alfvén se igualan. Esto es de suma relevancia, ya que en la transformación de modos se transmite de forma total o parcial energía de uno a otro lo que implica cambios en sus propiedades y en la forma de transportar la energía. En la parte final de la discusión de resultados estudiamos cómo dicha transformación de modos depende de varios parámetros que afectan a la cantidad de energía que se transmite. Los más importantes son el ángulo que forma el vector de onda con el campo magnético y la frecuencia de la onda.

Contents

1 Introduction

Resumen

El Sol es nuestra estrella más cercana y el estudio de sus características y procesos son de vital importancia, ya que además de ejercer una gran influencia en el clima terrestre, nos aporta un mayor conocimiento de la física del plasma mediante su estudio. Su atmósfera se subdivide en: la fotosfera, cromosfera, región de transición y corona. Cada una tiene unas características físicas bien diferenciadas, pero en la zona alta de la cromosfera, la región de transición y la corona se observa un gran aumento de las temperaturas. Este hecho observacional es uno de los principales problemas en física solar, puesto que considerando el mecanismo de transporte radiativo las temperaturas deberían de decrecer según nos alejamos de la superficie. Luego es necesario que se investiguen otros mecanismos de transporte en la atmósfera que lleguen a explicar dicho fenómeno, uno de ellos es la disipación de las ondas acústicas. En la atmósfera solar se propagan multitud de ondas que van desde las acústico-gravitatorias a las magneto-acústicas y, dependiendo de su modo, los mecanismos de liberación de energía varían. Por lo tanto, es de gran interés estudiar su caracterización física y propagación en este medio. Esta es la principal motivación del trabajo, en el cual centramos la atención en el análisis de las capas bajas de la atmósfera (fotosfera,cromosfera) y su región frontera (la región de equipartición) en la cual, como se verá más adelante, se podría producir una transferencia de energía entre distintos modos, lo que se conoce como transformación de modos.

1.1 Solar atmosphere

The Sun is our nearest star and has been the subject of study for more than 100 years because of its great importance in our daily lives. For example, it has a major influence on the Earth's climate and space weather. Some effects of solar activity on the Earth are auroras or those that can excite a geomagnetic storm in the Earth's magnetosphere, which can even damage satellite communication. Solar flares and coronal mass ejections (CMEs) are some of the events that produce them and have their origin in the solar atmosphere. These effects remark the importance of studying the dynamic processes occurring in the Sun and the changes in its atmosphere. Moreover, the solar atmosphere is in a plasma state, so its study can provide us with a better understanding of plasma physics and related plasma cosmical phenomena. Furthermore, due to its proximity, it facilitates the observation and study of stellar phenomena. The Sun is the only star whose surface we can observe in detail and is one of the most common stars in the universe (it is a G-type main sequence star).

The basic structure of the Sun is divided into the solar interior, which is shielded from our view due to the high opacity, and the solar atmosphere, from where the radiation we observe in the Earth is coming. The solar atmosphere is divided into several layers, mainly due to differences in their physical properties, such as density and temperature. The innermost layer, known as the photosphere, has an effective temperature of about 6000 K, since the light is emitted mainly in the visible range of the electromagnetic spectrum. In this layer, with a thickness of about 500km, we observe the sunspots (see left panel of Figure 1) and granulations. The layer above it is the chromosphere, where the temperature starts to grow again as we move to the upper layers, it is much less dense than the photosphere and it is dominated by magnetic forces. At the top of the chromosphere, the temperature increases dramatically through the transition region. This region is a quite thin layer compared to the other layers of the atmosphere, only a few kilometres thick. It separates the much cooler chromosphere from the extremely hot corona, increasing the temperature from 25000K to 10^6K. The outer layer, the corona, has extremely high temperatures, therefore an extremely high level of ionization of elements. And contains structures such as plumes and loops or events like the CMEs (Stix, 2004; Priest, 2014; Bhatnagar & Livingston, 2005).

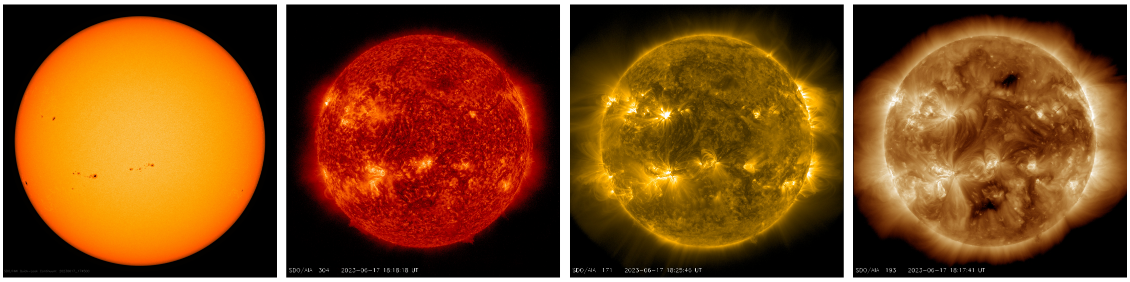

Figure 1: From left to right: an image of the photosphere in the continuum, 304 Å image of the chromosphere and the transition region emitted by He II, 171 Å image of the upper transition region and the corona emitted by Fe IX, 193 Å image of the corona emitted by Fe XII. Credits NASA/SDO (2023).

The present study focuses on the lower layers of the atmosphere, the photosphere and chromosphere. One of the most important properties that differentiate these layers is a dimensionless parameter β. It is the ratio of the gas pressure to the magnetic pressure. If $\beta \gg 1$ the magnetic field is not strong enough and plays a secondary role in the dynamics, so the plasma motion is more gas-like (photosphere). In the opposite case, the magnetic forces dominate the dynamics (chromosphere).

Related to these layers, one of the biggest problems in solar physics is the heating of the chromosphere and corona. As shown in Figure 2, the temperature rises abruptly in the transition and corona regions. The problem is that if radiation were the only energy transport mechanism in the solar atmosphere, it would lead to a negative temperature gradient. Therefore, another heating mechanism must be proposed.

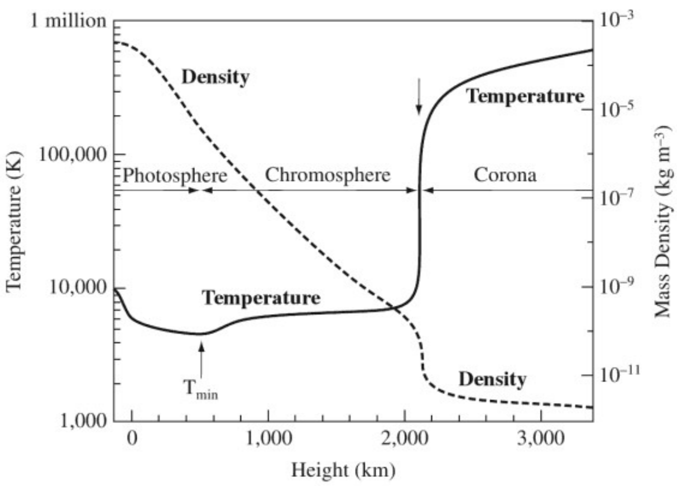

Figure 2: A schematic representation of the temperature and density observational profiles as a function of the height in the solar atmosphere (Priest, 2014).

Figure 2 also shows that the temperature in the lower part of the solar atmosphere varies in the range from 5000 K to 9000 K, which means that the gas is partially ionised. In this medium, which we refer to as plasma, different types of waves are propagating and can dissipate their energy. Then, one proposed solution to the chromospheric heating problem is the dissipation of acoustic waves that are generated in the convection zone and propagate upwards to the solar atmosphere (Biermann, 1946; Schwarzschild, 1948). In addition to acoustic waves, other kinds of waves can propagate in the solar atmosphere, like Alfvén or magnetoacoustic waves. Depending on the mode, the mechanisms for releasing energy into the medium vary. Therefore, the physical characterisation of modes is quite important factor in explaining chromospheric heating by wave dissipation.

1.2 Motivation of this work

This study focuses on understanding the behaviour of waves in the boundary region separating the photosphere-chromosphere and in both layers. The main objective is to characterise the propagation of magneto-acoustic waves and the changes of polarisation they experience in their vertical propagation from the photosphere to the chromosphere. These layers have different characteristics as mentioned previously, so a wave that goes from the photosphere to the chromosphere (or viceversa) will suffer a change in its properties. This may be applied to any region where there is such a change, like a sunspot. In the frontier of the photosphere-chromosphere, the equipartition region, the wavelengths of the modes become so close that they can interact. This could give rise to the phenomenon of mode conversion in which one mode transfers energy to another (Schunker & Cally, 2006).

In section 2, we present the ideal magnetohydrodynamic (MHD) equations that describe plasma dynamics to then use them to describe wave propagation in the plasma.

In section 3, we consider a simplified model of the atmosphere as a stratified and isothermal medium. Once the medium is characterised, we linearise the equations assuming that the magnetic field is not important. This allows us to present the linearisation method and the characteristics of acoustic waves and important frequencies in a simple way. Here, we first derive the dispersion relation for acoustic waves in a 1D. And then we derive the acoustic-gravity waves dispersion relation in 2D. In addition, we describe the characteristics of their propagations and the effects of the cut-off frequency and the Brunt-Väisälä frequency are discussed.

In section 4, the MHD equations are applied and linearised to derive the propagation characteristics of the magnetoacoustic waves. We start with a 3D problem and a homogenous medium to simplify the algebra. Then we reduce the problem to 2D ignoring the Alfvén waves and we obtain the dispersion matrix of the magnetoacoustic wave. Besides, we describe in detail the effects of the dominant forces in the plasma (magnetic or hydrodynamic) on these modes. Furthermore, we arrive at the energy conservation equation for magnetoacoustic waves and describe the conditions for these waves to conserve energy.

In section 5, the changes in the background quantities (pressure and density) due to height stratification are taken into account. Here, we present the ray tracing formalism for analysing wave propagation in a weakly inhomogeneous medium, as it simplifies the analysis. The results found in section 4 are applied, even though these have been found for a homogeneous atmosphere. Because considering high frequencies (higher than the Brunt-Väisälä and cut-off frequency) we can manipulate the same terms as in section 4, neglecting the gravity terms. And we treat the mode conversion phenomenon following the mathematical formalism of Tracy et al. (2014).

Finally, in section 6, we summarize and discuss the implications of these results.

2 MHD theory

Resumen

En esta segunda sección describimos el marco teórico en el que se desarrollará el posterior estudio de las ondas en la atmósfera solar. Se presentan las ecuaciones magnetohidrodinámicas (MHD) ideales, las cuales nos permiten estudiar el comportamiento del plasma bajo unas ciertas condiciones. Se describen las suposiciones y aproximaciones que se toman a la hora de llegar a las ecuaciones MHD ideales y se discute cómo éstas no tienen de forma explícita la presencia del campo eléctrico.

The solar atmosphere is mainly composed of hydrogen, which has an abundance of almost 80%. Due to the high temperatures in the low atmosphere, hydrogen is expected to be ionized and, therefore, the atmosphere is in a plasma state. A plasma is a fluid macroscopically neutral that contains many interacting electrons and ionized atoms or molecules to compensate the charge, and whose behaviour is collective. In plasmas, charge neutrality is not satisfied at spatial scales smaller than a Debye length. This is the spatial range in which a local charge imbalance produces an electrical field: $\lambda_D = (\epsilon_0 k_B T/(ne^2))^{1/2}$, where k_B is the Boltzmann constant, ϵ_0 the vacuum permittivity, T the temperature, n the electronic density and e the electron charge (Bittencourt, 2004).

As a consequence, to describe the dynamics we introduce the basic magnetohydrodynamics equations (MHD). In MHD, the macroscopic behaviour of a continuous plasma is described through a combination of Maxwell's laws and the hydrodynamic equations. The plasma can be treated as a continuum as long as the length scale of the variations exceeds greatly the internal plasma lengths. The basis in MHD is that magnetic fields can induce a current in the fluid and as a result, it can also change the magnetic field as well. Before discussing the hydrodynamic equations that form it, we present here the Maxwell equations[1]

$$\nabla \times \vec{B} = \mu_0 \vec{J} + \frac{1}{c^2}\frac{\partial \vec{E}}{\partial t}, \tag{1}$$

$$\nabla \times \vec{E} = -\frac{\partial \vec{B}}{\partial t}, \tag{2}$$

$$\nabla \cdot \vec{E} = \frac{\rho^*}{\epsilon_0}, \tag{3}$$

$$\nabla \cdot \vec{B} = 0. \tag{4}$$

The equations show the relation between the electromagnetic variables, where $\vec{B}$ is the magnetic field, $\vec{E}$ the electric field, $\vec{J}$ the current density, ρ^* the charge density, μ_0 is the vacuum magnetic permeability and c the speed of light. Equation (1), known as Ampère's law, tells us that temporal variations of the electric field and currents produce magnetic fields. Then, equation (2), known as Faraday's law of induction, shows that temporal variations of the magnetic field produce electric fields. Equations (3) and (4) are known as Gauss's law for the electric field and for magnetism, respectively. The former implies that charges are electric field sources. On the other hand, equation (4) indicates that the magnetic field has neither sources nor sinks; it is a solenoidal field. This equation assumes that there are no magnetic monopoles.

The plasma neutrality makes that $\rho^* \approx 0$, a necessary condition to apply the ideal MHD. In addition, relativistic effects can be neglected since the velocities associated with the plasma

[1] In the present work, the following mathematical notation is used: $\cdot$ for the scalar product, $\times$ vectorial product, $\otimes$ outer product, the $\vec{u}$ to denote vectors, $\hat{x}$ to denote unit vectors and $\bar{\bar{p}}$ to denote tensors

particles are typically much smaller than the speed of light. We also assume the plasma to behave as an ideal conductor, so it follows the ideal Ohm's law:

$$\vec{E} = -\vec{u} \times \vec{B}. \tag{5}$$

Substituting the previous expression into the induction equation (2) we remove the electric field explicitly and it results in

$$\frac{\partial \vec{B}}{\partial t} = \nabla \times (\vec{u} \times \vec{B}). \tag{6}$$

Moreover, under these conditions the current density is of the form:

$$\vec{J} = \frac{1}{\mu_0} \nabla \times \vec{B}. \tag{7}$$

With these expressions we can obtain hydrodynamic equations which are only determined by the magnetic field, hence the name MHD. This ideal approach leads to the magnetic field being frozen with the plasma itself (Priest, 2014). From now on, we are always going to deal with the ideal MHD approximation. The hydrodynamic equations that form the MHD are the following:

$$\frac{\partial \rho}{\partial t} + \nabla \cdot (\rho \vec{u}) = 0, \tag{8}$$

$$\frac{\partial}{\partial t}(\rho \vec{u}) + \nabla \cdot (\rho \vec{u} \otimes \vec{u} + \bar{\bar{p}}) = \vec{J} \times \vec{B} + \rho \vec{g}, \tag{9}$$

$$\frac{\partial}{\partial t}\left(e + \frac{1}{2}\rho u^2\right) + \nabla \cdot \left[\left(e + \frac{1}{2}\rho u^2\right)\vec{u} + \bar{\bar{p}} \cdot \vec{u}\right] = \vec{E} \cdot \vec{J} + \rho \vec{g} \cdot \vec{u}. \tag{10}$$

As we are in the ideal MHD approach, the heat flux $\vec{q}$ and viscosity ν terms have been neglected in the above equations. Equations (8), (9), and (10) are the mass continuity equation, the motion equation, and the energy equation, respectively, where ρ is the density of the plasma, $\vec{u}$ the velocity of the plasma, $\bar{\bar{p}}$ the stress tensor, e the internal energy and $\vec{g}$ the gravity. The scalar pressure p is $p = \frac{1}{3}\mathrm{Tr}(\bar{\bar{p}})$ and in the isotropic case $\bar{\bar{p}} = p\bar{\bar{I}}$. Furthermore, closure relations provide us with expressions that relate variables whose evolution we do not know, such as temperature T, with p and ρ as follows

$$p = \frac{\rho}{\tilde{\mu} m_H} k_B T, \tag{11}$$

$$e = \frac{p}{\gamma - 1}. \tag{12}$$

In the ideal gas law, equation (11), m_H is the mass of hydrogen, k_B is the Boltzmann constant, T is the temperature of the plasma and $\tilde{\mu}$ is the mean molecular weight. In a fully ionized hydrogen plasma $\tilde{\mu} = m/m_H = 0.5$ (where m is the average mass) and in an almost neutral atmosphere is $\tilde{\mu} \approx 1$. In the internal energy equation (12), γ is the adiabatic constant (for a monoatomic gas $\gamma = 5/3$).

Finally, taking into account all the approximations, we have the ideal MHD equations:

$$\frac{\partial \rho}{\partial t} = -\nabla \cdot (\rho \vec{u}), \tag{13}$$

$$\frac{\partial}{\partial t}(\rho \vec{u}) + \nabla \cdot (\rho \vec{u} \otimes \vec{u} + \bar{\bar{p}}) = (\nabla \times \vec{B}) \times \frac{\vec{B}}{\mu_0} + \rho \vec{g}, \tag{14}$$

$$\frac{\partial}{\partial t}\left(e + \frac{1}{2}\rho u^2\right) + \nabla \cdot \left[\left(e + \frac{1}{2}\rho u^2\right)\vec{u} + \bar{\bar{p}} \cdot \vec{u}\right] = \frac{1}{\mu_0}\left[(\nabla \times \vec{B}) \times \vec{B}\right] \cdot \vec{u} + \rho \vec{g} \cdot \vec{u}, \tag{15}$$

$$\frac{\partial \vec{B}}{\partial t} = \nabla \times (\vec{u} \times \vec{B}), \tag{16}$$

$$\nabla \cdot \vec{B} = 0. \tag{17}$$

Under the conditions explained previously for the plasma, this system of equations simplifies and brings together everything necessary for our study of plasma behaviour in the solar atmosphere. An interesting thing about the energy equation of this system is that if we rewrite it, eliminating the kinetic energy, we get that

$$\frac{\partial e}{\partial t} + \nabla(e\vec{u}) + p\nabla \cdot \vec{u} = 0. \tag{18}$$

This equation represents the evolution of the internal energy, which the magnetic field does not contribute to. It also does not contribute directly to the temperature evolution, as can be deduced from the closure relations. Furthermore, combining the continuity and the internal energy equations, that is, equations (13) and (18), and applying the relation (12) gives

$$\frac{D}{Dt}\left(\frac{p}{\rho^\gamma}\right) = 0, \tag{19}$$

where D/Dt is the Lagrange derivative[2]. This equation tells us that the value of p/ρ^γ (the adiabatic relation) does not change for a fluid element we are pursuing, so the processes described by these equations are adiabatic (Priest, 2014; Boyd et al., 2003; Bittencourt, 2004).

In the following sections, we will derive from equations (13)-(17) the properties of several types of waves that can propagate in the solar atmosphere. On the one hand, in section 3 we will neglect the effect of the magnetic field in order to focus on the linearisation method and the propagation of acoustic-gravitational waves in a stratified atmosphere. On the other hand, in section 4 the presence of the magnetic field will be taken into account to describe the properties of magnetoacoustic waves.

3 HD waves

Resumen

En esta sección se mostrará una primera visión de como se propagan las ondas en la atmósfera solar estratificada cuando no está presente el campo magnético o este no es importante. Aquí se muestra la derivación de las ecuaciones de onda mediante la linearización de las ecuaciones hidrodinámicas. Método el cual será utilizado en varias ocasiones durante el desarrollo del trabajo, a partir de estas ecuaciones conoceremos algunas características de las ondas acústicas y acústico-gravitatorias. Además, trataremos en detalle algunas frecuencias características de estas ondas, como son la frecuencia de corte y la frecuencia de Brunt Väisälä y finalizaremos discutiendo la conservación de la energía de las ondas acústico-gravitatorias.

Now that we have presented our theoretical framework for studying plasma dynamics, that is, the MHD model, let us focus on the propagation of waves in the solar atmosphere in the absence of magnetic terms. Therefore, here we neglect all the terms of equations (8)-(10) that depend on $\vec{B}$. This section gives a first, simple approach to the structure of the solar lower atmosphere (photosphere and chromosphere). Besides, it presents the main method to derive the linearised set of equations.

To study the propagation of a linear wave that follows this system of equations presented in section 2, it would be necessary to linearise them by using a small perturbation analysis. In this analysis, we consider an equilibrium situation and then we add to it a small perturbation, in which we only retain the linear terms due to the smallness of the perturbations. We assume an

[2]The Lagrange derivative of a scalar is defined as: $\frac{Dq}{Dt} = \frac{\partial q}{\partial t} + \vec{u} \cdot (\nabla q)$

atmosphere in static equilibrium $\vec{u_0} = 0$ and vertically stratified along the direction of gravity but uniform in the other directions. Therefore, our equilibrium variables only depend on z. To obtain the linearised set of equations, we split the variables into an equilibrium part and a perturbed one as follows:

$$\begin{cases} p = p_0(z) + p'(z,t), \\ \rho = \rho_0(z) + \rho'(z,t), \\ \vec{u} = \vec{u}_0 + \vec{u}' = \vec{u}'(z,t), \end{cases}$$

$$\begin{cases} |p'| \ll p_0, \\ |\rho'| \ll \rho_0, \\ |\vec{u}'| \ll c_s, \end{cases}$$

where equilibrium values are denoted by the subscript "0" and perturbations are represented by the primed variables. For the velocity, we have the special case that its condition of smallness is considered with respect to the sound speed c_s, which is given by:

$$c_s = \sqrt{\frac{p_0}{\rho_0}\gamma}. \tag{20}$$

The sound speed is the speed of propagation of acoustic waves, if the velocity is similar to it, we cannot ensure that pressure and density perturbations are small compared to the equilibrium values.

Let us see how these variables fulfil the equilibrium conditions. The equilibrium relation for the continuity equation (8) indicates that ρ_0 is constant in time. And the energy equation (10) indicates that p_0 follows the same condition. But the motion equation (9) becomes

$$\frac{dp_0}{dz} = -\rho_0 g. \tag{21}$$

The last equation is the hydrostatic equilibrium equation, where we choose as our z axis like $\vec{g} = -g\hat{z}$ (in the Sun $g = 274m/s^2$). Integrating the last equation follows:

$$\int dlnp_0 = \int \frac{\rho_0 g}{p_0} dz. \tag{22}$$

Now, we introduce the parameter

$$H = \frac{p_0}{\rho_0 g}, \tag{23}$$

which has units of distance and it is called the pressure scale height. Back to the integral (22), its solution is given by

$$p_0(z) = p_{eq} e^{-\int \frac{dz}{H(z)}}. \tag{24}$$

The last equation describes how the equilibrium pressure varies in a stratified medium. If we also consider that the atmosphere is isothermal, we can take H out of the integral, since it is constant under this assumption. It can be easily seen if we replace p with the ideal gas law (11),

$$H = \frac{k_B T}{g\tilde{\mu} m_H} = \frac{p}{\rho g} = const, \tag{25}$$

because $\tilde{\mu} m_H = const$, $k_B = const$ and the fluid is isothermal ($T = const$). In the same way, the sound speed will be constant too (20). Back to equation (24), it now has the form

$$p_0(z) = p_{00} e^{-\frac{z}{H}}, \tag{26}$$

which means that the pressure decreases exponentially with height where H marks the rate of such decay.

For the remaining of this work, we use the equilibrium model represented by Figure 3, which shows the variations of pressure and density with height corresponding to an isothermal atmosphere of temperature $T = (p\tilde{\mu}m_H)/(\rho k_B) = 5207.81\text{K}$ and a very low ionization degree (so $\tilde{\mu} \approx 1$).

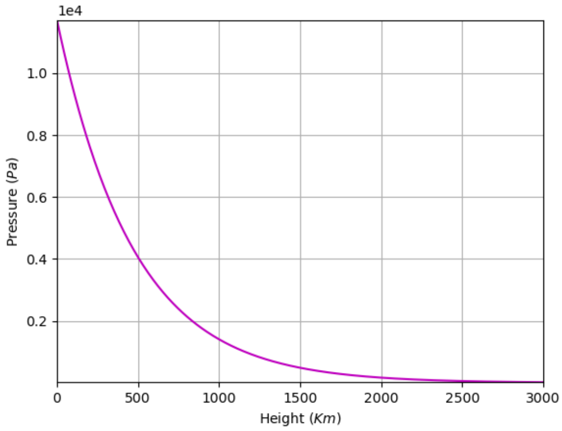

Figure 3: Pressure (left) and density (right) profiles as functions of height of our model atmosphere.

3.1 Wave propagation in a 1D, isothermal and stratified medium

Once we have the atmosphere described as a stratified, isothermal medium and with the equilibrium conditions determined, we can study the propagation of waves by linearising the equations. When we linearise equations we use the small perturbation analysis explained previously, in which we retain terms until first order. We are going to follow these steps throughout the study, but the algebra will be developed a little more in detail here than in the following sections.

We start linearising the continuity equation (8)

$$\frac{\partial(\rho_0 + \rho')}{\partial t} + \nabla \cdot (\rho_0 \vec{u}) + \nabla \cdot (\rho' \vec{u}) = 0.$$

Retaining up to linear terms only, that is, terms which are not a product of perturbations, we get

$$\frac{\partial \rho'}{\partial t} = -\frac{d\rho_0}{dz}u_z - \frac{\partial u_z}{\partial z}\rho_0.$$

Following the same steps for the momentum equation (9)

$$\frac{\partial}{\partial t}\left[(\rho_0 + \rho')u_z\right] + \frac{\partial}{\partial z}\left[(\rho_0 + \rho')u_z^2 + p_0 + p'\right] = -(\rho_0 + \rho')g$$
$$\Rightarrow \rho_0 \frac{\partial u_z}{\partial t} = -\frac{dp_0}{dz} - \frac{\partial p'}{\partial z} - \rho_0 g - \rho' g.$$

If we replace with equation (21) the motion equation is

$$\rho_0 \frac{\partial u_z}{\partial t} = -\frac{\partial p'}{\partial z} - \rho' g.$$

In the energy equation, we are going to introduce the closure relation (12):

$$\frac{\partial}{\partial t}\left(\frac{p_0 + p'}{\gamma - 1} + \frac{1}{2}(\rho_0 + \rho')u_z^2\right) + \frac{\partial}{\partial z}\left[\left(\frac{p_0 + p'}{\gamma - 1} + \frac{1}{2}(\rho_0 + \rho')u_z^2\right)u_z + (p_0 + p')u_z\right] = -(\rho_0 + \rho')gu_z.$$

Then, if we retain the linear terms we get

$$\frac{\partial}{\partial t}\left(\frac{p'}{\gamma-1}\right)+\frac{1}{\gamma-1}\left(\frac{dp_0}{dz}u_z+\frac{\partial u_z}{\partial z}p_0\right)+\frac{dp_0}{dz}u_z+\frac{\partial u_z}{\partial z}p_0=-\rho_0 g u_z$$
$$\Rightarrow \frac{\partial p'}{\partial t}+\gamma\left(\frac{dp_0}{dz}u_z+\frac{\partial u_z}{\partial z}p_0\right)=-(\gamma-1)\rho_0 g u_z$$

Replacing the term dp_0/dz with equation (21), we find

$$\frac{\partial p'}{\partial t}-\gamma\rho_0 g u_z+\gamma p_0\frac{\partial u_z}{\partial z}=-(\gamma-1)\rho_0 g u_z$$
$$\Rightarrow \frac{\partial p'}{\partial t}=-\gamma p_0\frac{\partial u_z}{\partial z}+\rho_0 g u_z.$$

Finally, the system of linear equations that describes the propagation of hydrodynamic waves in the stratified solar atmosphere is

$$\frac{\partial \rho'}{\partial t}=-\frac{d\rho_0}{dz}u_z-\frac{\partial u_z}{\partial z}\rho_0, \tag{27}$$
$$\rho_0\frac{\partial u_z}{\partial t}=-\frac{\partial p'}{\partial z}-\rho' g, \tag{28}$$
$$\frac{\partial p'}{\partial t}=-\gamma p_0\frac{\partial u_z}{\partial z}+\rho_0 g u_z. \tag{29}$$

In order to find the wave equation for the velocity, we take the time derivative of the motion equation (28)

$$\rho_0\frac{\partial^2 u_z}{\partial t^2}=-\frac{\partial}{\partial t}\frac{\partial p'}{\partial z}-g\frac{\partial \rho'}{\partial t}, \tag{30}$$

and the spatial derivative of the energy equation (29),

$$\frac{\partial}{\partial t}\frac{\partial p'}{\partial z}=-\gamma\left(\frac{dp_0}{dz}\frac{\partial u_z}{\partial z}+p_0\frac{\partial^2 u_z}{\partial z^2}\right)+g\frac{d\rho_0}{dz}u_z+g\frac{\partial u_z}{\partial z}\rho_0$$
$$\Rightarrow \frac{\partial}{\partial t}\frac{\partial p'}{\partial z}=-\gamma\left(-\rho_0 g\frac{\partial u_z}{\partial z}+p_0\frac{\partial^2 u_z}{\partial z^2}\right)+g\frac{d\rho_0}{dz}u_z+g\frac{\partial u_z}{\partial z}\rho_0. \tag{31}$$

Then, replacing equation (31) into equation (30) [3]

$$\rho_0\frac{\partial^2 u_z}{\partial t^2}=-(\gamma+1)\rho_0 g\frac{\partial u_z}{\partial z}+\gamma p_0\frac{\partial^2 u_z}{\partial z^2}-g\frac{d\rho_0}{dz}u_z-g\frac{\partial \rho'}{\partial t}$$
$$\Rightarrow \rho_0\frac{\partial^2 u_z}{\partial t^2}=-(\gamma+1)g\rho_0\frac{\partial u_z}{\partial z}+\gamma p_0\frac{\partial^2 u_z}{\partial z^2}-g\frac{d\rho_0}{dz}u_z+g\frac{d\rho_0}{dz}u_z+\frac{\partial u_z}{\partial z}\rho_0 g$$
$$\Rightarrow \rho_0\frac{\partial^2 u_z}{\partial t^2}=-\gamma\rho_0 g\frac{\partial u_z}{\partial z}+\gamma p_0\frac{\partial^2 u_z}{\partial z^2}.$$

Finally, the wave equation for the velocity is

$$\frac{\partial^2 u_z}{\partial t^2}=-\gamma g\frac{\partial u_z}{\partial z}+c_s^2\frac{\partial^2 u_z}{\partial z^2}. \tag{32}$$

For this equation, we can propose the same type of solutions of the homogeneous case (in which $g=0$). We can say this in the isothermal case because it is an equation in partial derivatives with constant coefficients. Then, proposing that the solution to this equation is given by

$$u_z=Ae^{i(kz-\omega t)}, \tag{33}$$

[3] To exchange the derivatives we use the Schwarz theorem.

where k is the wavenumber, ω is the frequency of the oscillation and A is its amplitude. It can be shown that the dispersion relation that describes the properties of the waves has the form

$$w^2 = \gamma gik + c_s^2 k^2. \tag{34}$$

We are interested in propagating waves, therefore our waves have a given frequency ω and k is obtained as a function of it. If we had fixed k, we would be considered a study for standing waves in which we excite a specific spatial scale. A standing wave oscillates in time, but its profile does not move; the amplitude of the oscillations in space is constant with respect to time at fixed points called nodes. These waves do not propagate energy.

So, if we solve equation (34) as k being a function of ω, we get the expression

$$k = \frac{-\gamma gi \pm \sqrt{-\gamma^2 g^2 + 4c_s^2\omega^2}}{2c_s^2}. \tag{35}$$

Once we have described the behaviour of k, if we go back to the wave solution (33), we have the description of the propagation of an oscillation

$$u_z = Ae^{k_{im}z}e^{i(k_r z - \omega t)}, \tag{36}$$

where we have separated k from equation (35) into its imaginary and real component, $k = k_r + ik_{im}$. The term $k_r = (\sqrt{-\gamma^2 g^2 + 4c_s^2\omega^2})/(2c_s^2)$ is associated with the real part of k and contributes to the oscillatory part of the solution (33). But $k_{im} = \gamma g/2c_s^2 = 1/2H$ that is associated with the imaginary part, contributes to the amplitude so that as the height increases, the amplitude of the wave grows (due to the sign of $-\gamma gi/2c_s^2$ in equation (35)). This behaviour is shown in Figure 4, which illustrates well how as the height increases, the amplitude of the wave increases too.

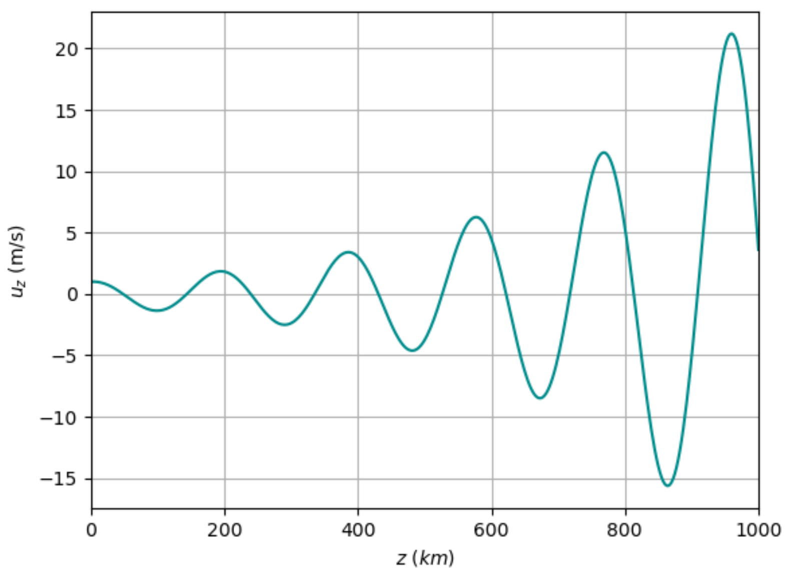

Figure 4: Analytical solution of a propagating wave increasing in amplitude with height, equation (36) with $g = 274m/s^2$, $\gamma = 5/3$, $\omega = 55$mHz and $c_s = 8463.414(m/s)$. The sound speed was calculated from the values of our atmosphere (Figure 3).

If k becomes pure imaginary, the solution (33) would change its behaviour and we would no longer have the propagation of a wave, it would be evanescent. An evanescent wave does not propagate, it decays exponentially with height:

$$u_z = Ae^{k_{im}z}e^{-i\omega t}. \tag{37}$$

Let us see when k becomes pure imaginary from equation (35). This occurs when we have a certain value of the frequency that fulfils the relation

$$\sqrt{-\gamma^2 g^2 + 4c_s^2\omega_c^2} = 0$$

$$\Rightarrow \omega_c = \frac{\gamma g}{2c_s}, \quad (38)$$

where ω_c is called cut-off frequency. If $\omega < \omega_c$, k becomes pure imaginary and our solution is an evanescent wave (37) and if $\omega > \omega_c$ the solution is related to a propagating wave (36). Figure 5 represents the behaviour of k given by equation (35). It shows that below the cut-off frequency, there is no solution for the propagation of a wave.

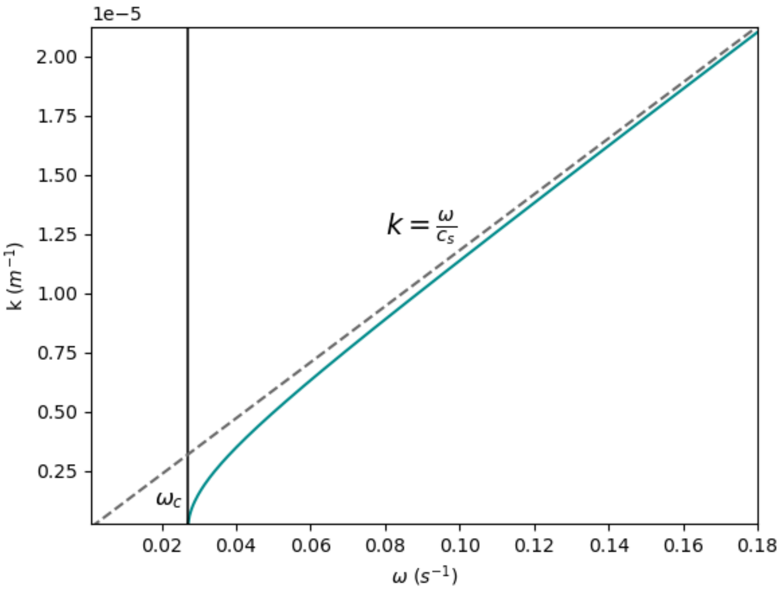

Figure 5: Wavenumber as a function of frequency for acoustic waves. The blue curve is the solution of equation (35), the dashed line is the solution for a homogeneous atmosphere and the vertical line represents the cut-off frequency (ω_c = 26.978 mHz, c_s = 8463.414m/s, g = 274m/s^2, $\gamma = 5/3$).

We conclude this subsection with the statement that in a stratified medium, acoustic waves present a cut-off frequency. As Figure 5 shows, as much the frequency approaches the cut-off frequency the value of k tends to zero since at lower values k is pure imaginary. Therefore, they cannot propagate, unlike the homogeneous case, which does not present this behaviour. We also note that as the frequency increases it approaches asymptotically to the homogeneous case.

3.2 Gravity waves

In the previous section, we have shown the wave solutions in a stratified and isothermal 1D atmosphere. And we observed how below the cut-off frequency acoustic waves cannot propagate. In this section, we will see that there are waves that do propagate at low frequencies, even below this cut-off frequency: they are called gravity waves. The purpose of this section is to illustrate the interpretation of the Brunt-Väisälä frequency and it follows the derivation of gravity waves from the book by Priest (2014).

First, we consider a blob of plasma in the absence of a magnetic field that is displaced vertically a distance δz from the equilibrium (Figure 6). The only external force is gravity. Now, we make two assumptions:

1. The blob remains in pressure equilibrium with its surroundings,
2. The density changes inside it are adiabatic.

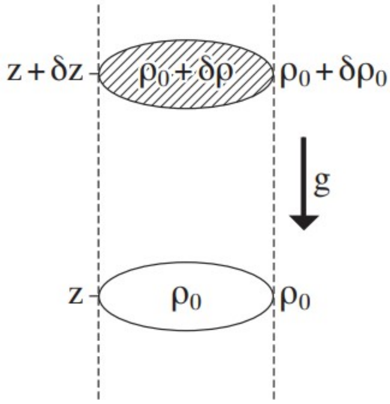

Figure 6: A blob of plasma that moves vertically against gravity from z to $z + \delta z$, where its surroundings present a density ρ_0 at height z and $\rho_0 + \delta\rho_0$ at $z + \delta z$ (Priest, 2014)

The first assumption is valid if the motion is so slow that sound waves can traverse the system faster than the time scale of interest. And to fulfil the second one, the motion has to be so fast that the entropy is preserved.

At the height z the fluid element is at equilibrium with the surroundings. Therefore, it satisfies the hydrostatic equilibrium equation (21). At height $z + \delta z$ the external medium has $p_0 + \delta p_0$, $\rho_0 + \delta\rho_0$, where the quantities with δ represent the changes in height, pressure and density with respect to the equilibrium quantities as the plasma element moves vertically. Replacing these expressions into equation (21) gives.

$$\delta p_0 = -\rho g \delta z, \tag{39}$$

$$\delta\rho_0 = \frac{d\rho_0}{dz}\delta z. \tag{40}$$

Inside the blob the pressure and density are $p_0 + \delta p$ and $\rho_0 + \delta\rho$ (at height $z + \delta z$) but, by the first assumption, the pressure inside the blob and the pressure of the external medium are equal. So,

$$\delta p = \delta p_0 = -\rho g \delta z.$$

And by the second assumption: $p/\rho^\gamma = const$, $\delta p/\delta\rho = \gamma(p_0/\rho_0) = c_s^2$. Therefore, $\delta p = c_s^2\delta\rho$. Substituting δp gives the internal density change as:

$$\delta\rho = -\frac{\rho_0 g \delta z}{c_s^2}. \tag{41}$$

The density inside the blob differs from the density of the surroundings, so at its new height, it experiences a buoyancy force:

$$g(\delta\rho_0 - \delta\rho) = -N^2\rho_0\delta z, \tag{42}$$

where N^2 is obtained by (39) and (41) equations,

$$N^2 = -g\left(\frac{1}{\rho_0}\frac{d\rho_0}{dz} + \frac{g}{c_s^2}\right). \tag{43}$$

When N is real, it is known as the Brunt-Väisälä frequency. It represents the frequency at which a vertically displaced blob from its equilibrium position will oscillate.

Generally, N varies with height, but when the temperature T_0 is uniform it becomes

$$N^2 = \frac{(\gamma - 1)g^2}{c_s^2}, \tag{44}$$

which is also constant.

As indicated previously, our atmosphere is isothermal, so this will be the form of N for our study.

If the only force acting on the fluid element is buoyancy, that is a force related to gravity, the equation of motion has the following form:

$$\rho_0 \frac{d^2(\delta z)}{dt^2} = -N^2 \rho_0 \delta z. \tag{45}$$

The last equation (45), is a homogeneous second order equation and when N^2 is constant (44) the solution is given by

$$\delta z(t) = \delta z_0 e^{i\sqrt{N^2}} \tag{46}$$

If $N^2 > 0$ the solutions are oscillations with N as frequency. If $N^2 < 0$ the solutions are exponential and not oscillatory. This leads us to expect that when $N^2 > 0$ gravity waves appeared. These waves cannot propagate faster than the Brunt-Väisälä frequency. Then it is necessary for these waves that $N^2 > 0$ and their frequency is $\omega \leq N$. This is discussed in more detail in the next subsection 3.3 from the dispersion relation of acoustic-gravity waves.

3.3 Acoustic-gravity waves

In the previous subsections, we studied wave propagation in a stratified and isothermal 1D atmosphere. We now extend this study to 2D. Here, we are going to study a combination of acoustic waves in a stratified medium (which cannot propagate below the cut-off frequency) and gravity waves (which propagate at low frequencies and are characterised by the Brunt-Väisälä frequency).

To this aim, we follow the same methodology of linearising the hydrodynamic equations, although now in the two-dimensional case. As we state at the beginning of section 3, the atmosphere is only stratified in the vertical direction $\hat{z}$, so in the horizontal direction $\hat{x}$ it is uniform. This makes the variables in the equilibrium the same as the ones presented in section 3 and the system of linearised equations quite easy to deduce due to their similarity with subsection 3.1. These equations are:

$$\frac{\partial \rho'}{\partial t} = -\rho_0 \nabla \cdot \vec{u} - \frac{d\rho_0}{dz} u_z, \tag{47}$$

$$\rho_0 \frac{\partial \vec{u}}{\partial t} = -\nabla p' - \rho' g \hat{z}, \tag{48}$$

$$\frac{\partial p'}{\partial t} = -\gamma p_0 \nabla \cdot \vec{u} - \rho_0 g u_z, \tag{49}$$

In order to obtain the wave equation, we follow the same steps that in subsection 3.1 (this derivation is shown in Appendix A), which results in the following expression:

$$\frac{\partial^2 \vec{u}}{\partial t^2} = c_s^2 \nabla(\nabla \cdot \vec{u}) - \hat{z}(\gamma - 1)g(\nabla \cdot \vec{u}) - g\nabla u_z. \tag{50}$$

The solution to equation (50) has the following form:

$$\vec{u} = \vec{A}e^{i(\vec{k}\cdot\vec{r}-\omega . t)} \tag{51}$$

By introducing the solution (51) in equation (50), we obtain the dispersion relation (see Appendix A)

$$\omega^2(\omega^2 - i\gamma g k_z) = -g^2k^2(\gamma-1) + (\gamma-1)g^2k_z^2 + c_s^2k^2\omega^2.$$

This equation referred to in the appendix as (A.11) can be further simplified in order to find an equation that gives more physical meaning. For this purpose, we introduce $\vec{k}'$ ($\vec{k}' = \vec{k} + \frac{i}{2H}\hat{z} = \vec{k} + \frac{i\gamma g}{2}\hat{z}, k'^2 = k^2 + \frac{\gamma^2 g^2}{4}$) and we get

$$\omega^2(\omega^2 - \omega_c^2) = (\omega^2 - N^2\sin^2\theta_g')k'^2c_s^2, \tag{52}$$

where θ_g' is the angle between $\vec{k}'$ and the vertical axis ($\sin^2\theta_g' = 1 - \frac{k_z'^2}{k'^2}$) that is shown in Figure 7. By definition the real value of k and k' are the same. The inclusion of $\vec{k}'$ simplifies the algebra and the physical interpretation since it causes the appearance of the cut-off frequency and Brunt-Väisälä frequency.

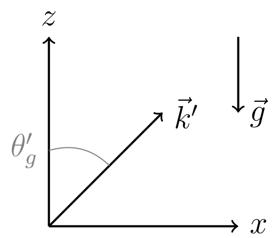

Figure 7: An illustration of the angle θ_g' that forms $\vec{k}'$ with the vertical axis z

Let us look at some of the characteristics of acoustic-gravity waves through the dispersion relation (52). When $\theta_g' = 0$ the expression reduces to $\omega^2 = \omega_c^2 + k'^2c_s^2$ and the wave propagates when $\omega > \omega_c$ (we recover the case of purely vertical propagation in subsection 3.1), therefore, gravity waves do not propagate in the vertical direction. The waves that propagate in the horizontal direction will have at higher frequencies, mainly acoustic nature and at lower frequencies, gravity nature.

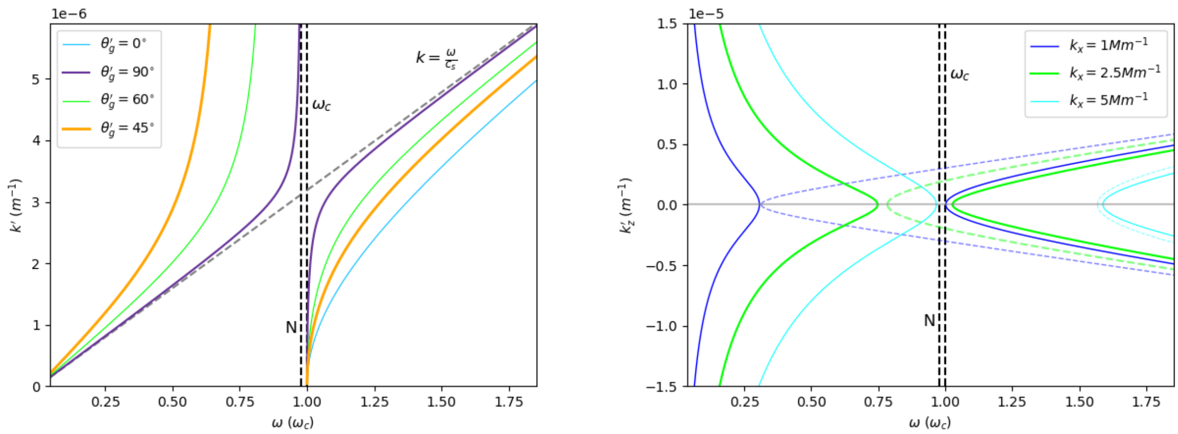

Figure 8: The change of k' (left) and k_z' (right) with frequency. They have the same parameters of Figure 5 and $N = 26.433$ mHz. The frequency is expressed in cut-off frequency units. Between the two black dashed lines (ω_c cut-off frequency and, N Brunt-Väisälä frequency) there is no real solution for k' and k_z' (evanescent waves). For the right figure, we fix different values for k_x' where the grey dashed lines represent k_z' for a homogeneous atmosphere.

We can observe in the left panel of Figure 8 that when the frequency is near to N, the value of k' tends to infinite; on the contrary, when the frequency is near to ω_c, k' tends to zero. This means that at frequencies close to Brunt-Väisälä the wavelength tends to zero and close to the cut-off frequency to infinite. In addition, the k' solution in Figure 8 shows that when $\theta_g = 0$ we recover the solution presented in Figure 5, as we previously deduced. In contrast, the right panel of Figure 8 shows the change of k'_z with the frequency. In this case, in order to be able to represent this change, it is necessary to fix k'_x. This is possible and logical since our atmosphere is stratified in the vertical direction (z) and homogeneous in the horizontal direction (x). This means, that there is no dependence on x, so k'_x remains constant. Therefore, starting from (52), we can obtain k'_z as a function of ω:

$$k_z'^2 = \frac{(\omega^2 - \omega_c^2)}{c_s^2} + \frac{N^2 k_x'^2}{\omega^2} - k_x'^2. \tag{53}$$

From the last equation, we can draw similar conclusions to the ones we derived for k'. At high frequencies, the term associated with the Brunt-Väisälä frequency can be neglected, and the wave becomes basically acoustic. And at low frequencies, a gravity wave. But unlike k', setting k'_x causes the wave to stop propagating in the vertical direction at higher frequencies, in the case of frequencies lower than Brunt-Väisälä, and at lower frequencies in the case of frequencies higher than the cut-off frequency. The last point can be observed in the right panel of Figure 8.

The inclusion of more dimensions in the study produces new normal modes. We have now two different normal modes, which are commonly known as the p mode (on the right of the cut-off frequency) and the g mode (on the left of the Brunt-Väisälä frequency) (Priest, 2014). The following paragraphs include a brief description of the modes.

On the one hand, p modes are essentially acoustic waves (or pressure waves) where the dominant restoring force is pressure. Acoustic waves propagate due to an interplay between density and velocity variations effected through the pressure term. A local compression or rarefaction of the fluid sets up a pressure gradient in opposition to the motion, which tries to restore the original equilibrium. In detail, acoustic waves are isotropic, compressive and longitudinal. This type of waves can be generated, e.g., in the Sun's convection zone by turbulent motions (Clarke & Carswell, 2007; Bhatnagar & Livingston, 2005; Goossens, 2003).

On the other hand, the dominant restoring force of g modes is buoyancy, and the modes have the character of standing internal gravity waves due to reflections when it propagates upwards, in a similar way, as can be seen in the solution of k_z in Figure 8 with the frequency. This mode is trapped in the solar interior and is exponentially damped in the outermost layers. In fact, they have their largest amplitude close to the solar centre. They are much more slowly propagating waves than the p modes. The internal gravity waves are found to be markedly anisotropic. Gravity is necessarily always in one particular direction, so there is no reason for isotropy (Lighthill, 2001; Christensen-Dalsgaard, 2002).

In the next section, we continue with the same methodology, but we are going to consider a homogeneous atmosphere and we are going to include the magnetic field. However, before concluding this section, let us see if acoustic gravity waves preserve energy.

3.3.1 Energy conservation

One of the most important things in physics is energy conservation. To check that acoustic-gravity waves conserve energy during their propagation, first we have to obtain the expression for the energy associated with the waves, which will be quadratic and in a conservative form. An equation in conservative form is

$$\frac{\partial e}{\partial t} + \nabla \cdot \vec{F} = 0, \tag{54}$$

which is like the continuity equation (13). To find the energy conservative equation, we have to do a little algebra. Taking the scalar product with $\vec{u}$ in the momentum equation (48) we obtain

$$\frac{\partial}{\partial t}\left(\frac{1}{2}\rho_0 u^2\right) = -\vec{u}\cdot\nabla p' - u_z\rho' g$$
$$\Rightarrow \frac{\partial}{\partial t}\left(\frac{1}{2}\rho_0 u^2\right) = -\nabla\cdot(p'\vec{u}) + p'\nabla\cdot\vec{u} - u_z\rho' g. \tag{55}$$

Then, we introduce the displacement vector $\vec{\xi}$ of a plasma element away from the equilibrium state (Goedbloed & Poedts, 2004), which follows equation

$$\frac{\partial\vec{\xi}}{\partial t} + (\vec{u}\cdot\nabla)\vec{\xi} = \vec{u}. \tag{56}$$

In the linearised regime, the displacement vector is given by

$$\frac{\partial\vec{\xi}}{\partial t} \approx \vec{u}. \tag{57}$$

We now introduce $\vec{\xi}$ into equation (49) but only for the gravity terms. In order to group them into the temporal derivative.

$$\frac{\partial}{\partial t}\left(\frac{p'}{p_0\gamma} - \frac{\rho_0}{p_0\gamma}g\xi_z\right) = -\nabla\cdot\vec{u}. \tag{58}$$

The displacement is introduced without the perturbed label because it is related to $\vec{u}$ and the velocity is not denoted with the perturbed label since $u_0 = 0$, so we do not denote ξ as such either. Then, we replace $\nabla\cdot\vec{u}$ in the continuity equation (48) by the relation above:

$$\frac{\partial\rho'}{\partial t} = \frac{\partial}{\partial t}\left(\frac{p'}{c_s^2} - \frac{\rho_0}{c_s^2}g\xi_z - \frac{d\rho_0}{dz}\xi_z\right). \tag{59}$$

Finally, eliminating the temporal derivative, substituting these terms in equation (55) and using the definition of the Brunt-Väisälä frequency, equation (43), we obtain an energy equation in conservative form:

$$\frac{\partial}{\partial t}\left(\frac{1}{2}\rho_0 u^2 + \frac{p'^2}{2c_s^2\rho_0} + \rho_0 N^2\xi_z^2\right) + \nabla\cdot(p'\vec{u}) = 0. \tag{60}$$

The first term is the kinetic energy associated with the plasma velocity, whilst the second term is the pressure energy, sometimes called "elastic energy" (Bray & Loughhead, 1974). These two terms will appear even in the absence of gravity (Landau & Lifshitz, 2013). However, the third term with the Brunt-Väisälä frequency appears due to the contribution of gravity. It is the buoyancy energy and is termed by Eckart (2013) as the "thermobaric" energy. The term $p'\vec{u}$ represents the wave energy flux vector. In order to simplify the expression we can define e'_{tot} as

$$e'_{tot} = \frac{1}{2}\rho_0 u^2 + \frac{p'^2}{2c_s^2\rho_0} + \rho_0 N^2\xi_z^2. \tag{61}$$

Finally, we interpret the energy conservation equation using a fixed control volume and we check under which conditions energy is conserved. A fixed control volume V_{cont} is a certain volume whose boundaries do not change on time, i.e., instead of following a plasma element in time we choose a volume that does not change in time. Now, if we integrate equation (60) in this volume:

$$\int_{V_{cont}} \left[\frac{\partial e'_{tot}}{\partial t} + \nabla \cdot (p'\vec{u}) \right] dV = 0. \tag{62}$$

Our volume, V_{cont}, remains fixed as time advances so is a fixed mathematical domain for the integral and we can pull the partial temporal derivative out of the integral as a total derivative[4]:

$$\frac{d}{dt} \int_{V_{cont}} e'_{tot} dV = - \int_{V_{cont}} \nabla \cdot (p'\vec{u})\, dV. \tag{63}$$

Using Gauss divergence theorem and calling $\hat{n}$ the outward unit vector of the surface, we get

$$\frac{d}{dt} \int_{V_{cont}} e'_{tot} dV = - \oint_{\partial V_{cont}} p'\vec{u} \cdot \hat{n}\, dS, \tag{64}$$

where ∂V_{cont} is the surface of the volume V_{cont} and the right hand side is a close integral. The right term becomes zero when the scalar product $\vec{u} \cdot \hat{n} = 0$, i.e., when the vectors are orthogonal to each other. If the scalar product is zero we force that the integral becomes zero independently of the control volume. The last point is important because if the energy were to grow over time, the quantities inside the volume would eventually diverge and the model would lose predictability. This is more a necessity of the model but it is still true in the vast majority of cases. Therefore, if the right term of equation (64) is zero

$$\frac{d}{dt} \int_{V_{cont}} e'_{tot} dV = 0 \tag{65}$$

$$\Rightarrow E'_{tot} = const, \tag{66}$$

where we define E'_{tot} as the total energy contained in the volume:

$$E'_{tot} = \int_{V_{cont}} e'_{tot}\, dV. \tag{67}$$

In conclusion, if the boundary conditions allow the scalar product to be $\vec{u} \cdot \hat{n} = 0$, the acoustic-gravity waves preserve the energy.

4 MHD waves

Resumen

En esta sección hacemos uso de las ecuaciones MHD en 3D, con ellas se procederá a ver las características principales de las ondas de Alfvén y las magnetoacústicas. Para las ondas magnetoacústicas se presentará un sistema de referencia adecuado que nos permite simplificar el álgebra, ya que pasamos de 3D a 2D. A partir de aquí derivaremos la relación de dispersión para las ondas magnetoacústicas, describiremos sus características y direcciones de polarización de los dos modos que la componen. Estudiaremos a partir de estos resultados las propiedades de cada modo según el medio donde se encuentren, es decir, en la fotosfera (cuando dominan los términos hidrodinámicos) o en la cromosfera (cuando dominan las fuerzas magnéticas). Con el estudio de estos límites se observará cómo estos modos poseen algunas de las características de las ondas estudiadas con anterioridad. Por último, también describiremos las condiciones para que las ondas magnetoacústicas conserven la energía

[4] Leibniz's rule expresses the derivative of an integral like $\frac{d}{dx}(\int_{a(x)}^{b(x)} f(x,t)dt)$ in one that includes the evaluated functions multiplied by the derivative of the limits ($a(x)$ and $b(x)$) and a partial derivative inside the integral. In the particular case of an integral that is in a fixed domain, it simplifies to the case shown in the main text.

We will now begin the study of the waves that we will mainly deal with, those involving the ideal MHD equations. The previous sections have provided familiarity with the linearisation method, as well as important characteristics of some of the waves propagating through the solar atmosphere like the effects of the Brunt-Väisälä and cut-off frequencies. In this section, we include the magnetic field and a 3D configuration, but to simplify the calculations we consider the atmosphere to be homogeneous. Furthermore, we consider that the magnetic field is homogeneous. Therefore, we have that all equilibrium coefficients are homogeneous:

$$\begin{cases} p = p_0 + p', \\ \rho = \rho_0 + \rho', \\ \vec{u} = \vec{u}', \\ \vec{B} = \vec{B}_0 + \vec{B}'. \end{cases}$$

The linearised equations are (a detailed derivation of the equations is shown in Appendix B)

$$\frac{\partial \rho'}{\partial t} = -\rho_0 \nabla \cdot \vec{u}, \tag{68}$$

$$\rho_0 \frac{\partial \vec{u}}{\partial t} = -\nabla p' + (\nabla \times \vec{B}') \times \frac{\vec{B}_0}{\mu_0}, \tag{69}$$

$$\frac{\partial p'}{\partial t} = -\gamma p_0 \nabla \cdot \vec{u}, \tag{70}$$

$$\frac{\partial \vec{B}'}{\partial t} = \nabla \times (\vec{u} \times \vec{B}_0), \tag{71}$$

$$\nabla \cdot \vec{B}' = 0. \tag{72}$$

Unlike the hydrodynamic equations, here we have a system of five equations with the incorporation of the induction equation and Gauss's law for magnetism. Following the same procedure as in the previous sections (see Appendix B), the wave equation for the velocity is

$$\frac{\partial^2 \vec{u}}{\partial t^2} = c_s^2 \nabla(\nabla \cdot \vec{u}) + \left[\nabla \times (\nabla \times (\vec{u} \times \vec{B}_0))\right] \times \frac{\vec{B}_0}{\mu_0 \rho_0}. \tag{73}$$

If we compare this equation with the one presented in section 3.3, equation (50), we can observe that the term associated with the acoustic waves remains the same. However, the inclusion of the magnetic field has generated new terms that will change the nature of wave propagation. In addition, the vectors we are working with are now 3D, as opposed to those we were working with in section 3.3, which were 2D. Equation (73) admits the wave solution (51). Then, the dispersion relation is

$$\omega^2 \vec{u} = c_s^2 \vec{k}(\vec{k} \cdot \vec{u}) + \left[\vec{k} \times (\vec{k} \times (\vec{u} \times \vec{B}_0))\right] \times \frac{\vec{B}_0}{\mu_0 \rho_0}. \tag{74}$$

This last equation can be rewritten using the vectorial identity $(\vec{a} \times \vec{b}) \times \vec{c} = \vec{b}(\vec{a} \cdot \vec{c}) - \vec{a}(\vec{b} \cdot \vec{c})$, and doing some algebra (it is derived in the appendix as equation (B.13)) we get

$$\omega^2 \vec{u} = c_s^2 \vec{k}(\vec{k} \cdot \vec{u}) - \vec{B}_0(\vec{k} \cdot \vec{u}) \left(\vec{k} \cdot \frac{\vec{B}_0}{\mu_0 \rho_0}\right) + \frac{\vec{u}}{\mu_0 \rho_0}(\vec{k} \cdot \vec{B}_0)^2 + \vec{k}\frac{B_0^2}{\mu_0 \rho_0}(\vec{k} \cdot \vec{u}) - \vec{k}(\vec{k} \cdot \vec{B}_0)\frac{(\vec{B}_0 \cdot \vec{u})}{\mu_0 \rho_0}. \tag{75}$$

If we take that α is the angle that forms the magnetic field $\vec{B}_0$ with the wave vector $\vec{k}$ ($\vec{k} \cdot \vec{B}_0 = k B_0 \cos \alpha$), called the *attack angle* (Schunker & Cally, 2006), we find

$$\omega^2 \vec{u} = c_s^2 \vec{k}(\vec{k} \cdot \vec{u}) - \frac{B_0 k}{\mu_0 \rho_0} \cos \alpha \vec{B}_0(\vec{k} \cdot \vec{u}) + v_A^2 k^2 \cos^2 \alpha \, \vec{u} + v_A^2 \vec{k}(\vec{k} \cdot \vec{u}) - \frac{B_0 k}{\mu_0 \rho_0} \cos \alpha \, \vec{k}(\vec{B}_0 \cdot \vec{u}), \tag{76}$$

where

$$v_A = \frac{B_0}{(\mu_0 \rho_0)^{1/2}}, \tag{77}$$

is the called Alfvén velocity. Equation (76) depends only on the direction of the vectors $\vec{u}$, $\vec{B}_0$ and $\vec{k}$ and it has two different scalar products $\vec{B}_0 \cdot \vec{u}$ and $\vec{k} \cdot \vec{u}$. In the following sections we study the different dispersion relations that are obtained when both scalar products are zero, one of them is zero or the more general case, where neither of the products cancels out. This last case is the one in which we will go deeper into the description of its waves.

4.1 Alfvén waves

First, let us study the case in which the two scalar products in equation (76) are $\vec{B}_0 \cdot \vec{u} = 0$, $\vec{k} \cdot \vec{u} = 0$, meaning that both $\vec{B}_0$ and $\vec{k}$ are orthogonal to $\vec{u}$, so the velocity perturbation is normal to the plane determined by $\vec{B}_0$ and $\vec{k}$ (Figure 9). Therefore, we obtain a dispersion relation for this velocity component that is out of the plane and it is independent of the other components. The dispersion relation is

$$\omega = k v_A \cos\alpha. \tag{78}$$

This is the Alfvén dispersion relation, it is characterised as incompressible because if we take into account $\vec{k} \equiv \nabla$ and the relation $\vec{k} \cdot \vec{u} = 0$ leads to $\nabla \cdot \vec{u} = 0$ which is an expression related to incompressibility. Incompressibility implies that there are no variations in density and pressure of the fluid, as can be seen in equations (68) and (70) (with the incompressibility condition $\nabla \cdot \vec{u} = 0$). In other words, there are no compressions or decompressions in the fluid, unlike in acoustic waves, which is why they are also known as pressure waves because they cause a perturbation in pressure and density. So, Alfvén waves are transverse and magnetic in nature.

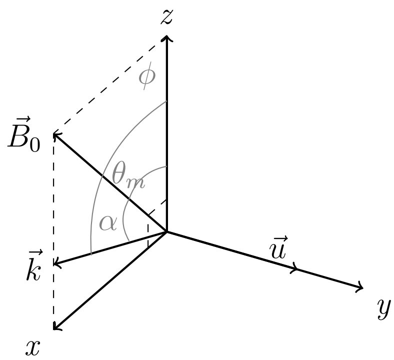

Figure 9: Sketch of the plane where $\vec{B}_0$ and $\vec{k}$ coexist, θ_m is the angle that $\vec{B}_0$ makes with respect to the z axis, α is the *attack angle* that $\vec{B}_0$ makes with respect to $\vec{k}$ and ϕ the angle that $\vec{k}$ forms with z axis.

Moreover, it can be shown that when $\vec{B}_0$ and $\vec{k}$ are parallel, we go from 3D to 2D. This is because $\vec{B}_0$ and $\vec{k}$ go from forming a plane to being contained in the same dimension. Therefore, we will have a plane formed by the direction of these two vectors and the orthogonal to it, where Alfvén waves are polarised, i.e., a 2D problem.

Now, we continue with the other possible cases of the dispersion relation (76). First, let us study the case where $\vec{k} \cdot \vec{u} = 0 \Rightarrow \vec{B}_0 \cdot \vec{u} = 0$, but not the other way around. In equation (76) we take the condition that $\vec{k} \cdot \vec{u} = 0$ (incompressibility condition):

$$\omega^2 \vec{u} = \frac{B_0^2 k^2}{\mu \rho_0} \cos^2\alpha \vec{u} - \frac{B_0 k}{\mu_0 \rho_0} \cos\alpha \vec{k} (\vec{B}_0 \cdot \vec{u}).$$

Then, we take the scalar product with $\vec{B_0}$:

$$\omega^2(\vec{B_0}\cdot\vec{u}) = \left(\frac{B_0^2k^2}{\mu\rho_0}\cos^2\alpha - \frac{B_0^2k^2}{\mu\rho_0}\cos^2\alpha\right)(\vec{B_0}\cdot\vec{u})$$
$$\Rightarrow \vec{B_0}\cdot\vec{u} = 0.$$

If the term $\vec{k}\cdot\vec{u} = 0$ implies that $\vec{B_0}\cdot\vec{u} = 0$.

Now let us see what happens in the case where $\vec{B_0}\cdot\vec{u} = 0$ and $\vec{k}\cdot\vec{u} \neq 0$:

$$\omega^2\vec{u} = \left(c_s^2\vec{k} - \frac{B_0 k}{\mu_0\rho_0}\cos\alpha\vec{B_0} + \frac{B_0^2k^2}{\mu_0\rho_0}\right)(\vec{k}\cdot\vec{u}).$$

Taking the scalar product with $\vec{k}$

$$\omega^2(\vec{k}\cdot\vec{u}) = (c_s^2k^2 - v_A^2\cos^2\alpha + v_A^2\cos^2\alpha + v_A^2k^2)(\vec{k}\cdot\vec{u})$$
$$\Rightarrow \omega^2 = c_s^2k^2 + v_A^2k^2. \tag{79}$$

We obtain one of the modes that compound the magnetoacoustic waves. We are going to discuss this mode in the next section, where we obtain the dispersion relation when none of the scalar products are zero.

In summary, Alfvén waves are magnetic waves whose polarisation direction is perpendicular to the plane of $\vec{B_0}$ and $\vec{k}$ and for this, Alfvén waves are not appearing in a 2D atmosphere where $\vec{B_0}$ and $\vec{k}$ coexist. This plane contains information of magnetoacoustic waves. In the following section, we study the dispersion relation of waves propagating in this plane which we consider to be at x and z axis.

4.2 Magnetoacoustic waves

From the previous section, we knew the characteristics of Alfvén waves that are polarised perpendicularly to the plane of $\vec{B_0}$ and $\vec{k}$. Therefore, we now study in detail the characteristics of magnetoacoustic waves whose information is in this plane. To do this, we continue with the case when none of the scalar products in equation (76) are zero. First, we take the scalar product with $\vec{k}$ in equation (76)

$$\left(\omega^2 - c_s^2k^2 - \frac{B_0^2k^2}{\mu_0\rho_0}\right)(\vec{k}\cdot\vec{u}) = -\frac{B_0k^3}{\mu_0\rho_0}\cos\alpha(\vec{B_0}\cdot\vec{u}). \tag{80}$$

Then taking the scalar product with $\vec{B_0}$

$$\omega^2(\vec{B_0}\cdot\vec{u}) = c_s^2B_0k\cos^2\alpha(\vec{k}\cdot\vec{u}). \tag{81}$$

Dividing these two equations (80), (81). Lead us to

$$\omega^4 - \omega^2k^2(c_s^2 + v_A^2) + v_A^2c_s^2k^4\cos^2\alpha = 0. \tag{82}$$

Finally, the previous biquadratic equation (82) has two solutions which are the two modes of magnetoacoustic waves:

$$k = \omega\left[\frac{(c_s^2 + v_A^2)}{2} \pm \frac{\sqrt{c_s^4 + v_A^4 - 2v_A^2c_s^2\cos 2\alpha}}{2}\right]^{-1/2}. \tag{83}$$

These two modes are the fast and slow, they are named after the relationship between their phase velocities. the phase velocity is the speed at which a wave propagates is given by ω/k.

The one with the higher value is the fast mode and the other one is the slow mode. When $\alpha = 90°$ the slow mode disappears and the fast mode becomes $k = \omega(c_s^2 + v_A^2)^{-1/2}$, we recover expression (79). When $\vec{B}_0 \parallel \vec{k}$ the solution becomes:

$$k = \omega \left[\frac{c_s^2 + v_A^2}{2} \pm \frac{c_s^2 - v_A^2}{2} \right]^{-1/2} \quad (84)$$

So, when $\alpha = 0°$ the solution to equation (83) is $\omega = kc_s$ or either $\omega = kv_A$.

The wave vector $\vec{k}$ can be decomposed in a perpendicular $k_\perp$ and parallel terms $k_\parallel$ with respect to the magnetic field (Figure 10) because we can ignore Alfvén waves by suppressing the $\hat{y}$ direction (we discussed this transition from 3D to 2D in the previous section). Therefore we now refer to 2D vectors (our new reference system has $k_y = 0$). This change of coordinates is given by

$$\begin{pmatrix} k_\parallel \\ k_\perp \end{pmatrix} = R(\theta_m) \begin{pmatrix} k_x \\ k_z \end{pmatrix}, \quad (85)$$

where $R(\theta)$ is the rotation matrix:

$$R(\theta_m) = \begin{pmatrix} \sin\theta_m & \cos\theta_m \\ \cos\theta_m & -\sin\theta_m \end{pmatrix}. \quad (86)$$

The decomposition of $\vec{k}$ is going to be useful in the next section, in which we use this new reference system to express the dispersion relation in matrix form. In order to find the direction of the polarisation vectors and to know in detail the characteristics of the fast and slow modes.

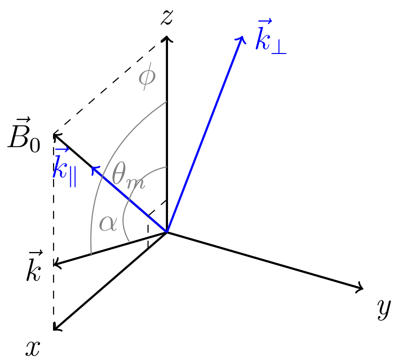

Figure 10: The decomposition of $\vec{k}$ into its perpendicular and parallel components. In this frame of reference in which $\vec{B}_0$ and $\vec{k}$ co-exist in the same plane, the Alfvén waves do not produce a velocity perturbation, since they are associated with the u_y component. Therefore, we can simplify the calculations.

4.2.1 Dispersion matrix, polarisation vectors and limits

We already have the dispersion relation of the magnetoacoustic waves for the fast and slow modes, but in order to know in which direction are they polarised, we can express the dispersion relation in matrix form and then diagonalise it. The eigenvalues are associated with the dispersion relation of each of the modes and their eigenvectors will indicate the direction of the velocity perturbation since they are linear combinations of the velocities. The eigenvectors are known in wave theory as polarisation vectors. So, let us first express the dispersion matrix from equation (75) (the derivation of the dispersion matrix and its diagonalisation can be found in Appendix C)

$$\begin{pmatrix} c_s^2 k_x^2 + v_A^2 k^2 \cos^2\theta_m - \omega^2 & c_s^2 k_x k_z - v_A^2 k^2 \sin\theta_m \cos\theta_m \\ c_s^2 k_x k_z - v_A^2 k^2 \cos\theta_m \sin\theta_m & c_s^2 k_z^2 + v_A^2 k^2 \sin^2\theta_m - \omega^2 \end{pmatrix} \begin{pmatrix} u_x \\ u_z \end{pmatrix} = 0, \quad (87)$$

where the dispersion matrix is

$$D = \begin{pmatrix} c_s^2 k_x^2 + v_A^2 k^2 \cos^2\theta_m - \omega^2 & c_s^2 k_x k_z - v_A^2 k^2 \sin\theta_m \cos\theta_m \\ c_s^2 k_x k_z - v_A^2 k^2 \cos\theta_m \sin\theta_m & c_s^2 k_z^2 + v_A^2 k^2 \sin^2\theta_m - \omega^2 \end{pmatrix}. \tag{88}$$

Then we diagonalise[5] D:

$$\begin{vmatrix} c_s^2 k_x^2 + v_A^2 k^2 \cos^2\theta_m - \omega^2 - \lambda & c_s^2 k_x k_z - v_A^2 k^2 \sin\theta_m \cos\theta_m \\ c_s^2 k_x k_z - v_A^2 k^2 \cos\theta_m \sin\theta_m & c_s^2 k_z^2 + v_A^2 k^2 \sin^2\theta_m - \omega^2 - \lambda \end{vmatrix} = 0$$

$$\Rightarrow \lambda = \frac{-2\omega^2 + (c_s^2 + v_A^2)k^2}{2} \pm k^2 \frac{\sqrt{(c_s^2 + v_A^2)^2 - 4c_s^2 v_A^2 \cos^2\alpha}}{2}, \tag{89}$$

where $\cos\alpha = \frac{k_\parallel}{k}$ (Figure 10). As explained in subsection 3.1, we are interested in wave propagation, so ω is fixed. Then, it can be said that the modes that will propagate will be those whose eigenvalue is zero. These eigenvalues are the ones associated with the slow and fast modes. Now, we can obtain the velocity polarisation of the fast and slow modes by calculating their eigenvectors. We start with the fast mode whose eigenvalue we denote as λ_f:

$$\begin{pmatrix} c_s^2 k_x^2 + v_A^2 k^2 \cos^2\theta_m - \omega^2 & c_s^2 k_x k_z - v_A^2 k^2 \sin\theta_m \cos\theta_m \\ c_s^2 k_x k_z - v_A^2 k^2 \cos\theta_m \sin\theta_m & c_s^2 k_z^2 + v_A^2 k^2 \sin^2\theta_m - \omega^2 \end{pmatrix} \begin{pmatrix} C_x^f \\ C_z^f \end{pmatrix} = \lambda_f \begin{pmatrix} C_x^f \\ C_z^f \end{pmatrix}$$

$$\Rightarrow C_x^f(\lambda_f - c_s^2 k_x^2 + \omega^2 - v_A^2 k^2 \cos^2\theta_m) = C_z^f(c_s^2 k_x k_z - v_A^2 k^2 \cos^2\theta_m \sin^2\theta_m)$$
$$\Rightarrow C_x^f = \frac{(c_s^2 k_x k_z - v_A^2 k^2 \cos\theta_m \sin\theta_m)}{\lambda_f - c_s^2 k_x^2 + \omega^2 - v_A^2 k^2 \cos^2\theta_m} C_z^f.$$

In order to determine the coefficients of the eigenvector we need another equation. Therefore, we take the normalisation condition

$$\frac{(c_s^2 k_x k_z - v_A^2 k^2 \cos\theta_m \sin\theta_m)^2}{(\lambda_f - c_s^2 k_x^2 + \omega^2 - v_A^2 k^2 \cos^2\theta_m)^2} |C_z^f|^2 + |C_z^f|^2 = 1$$

Then the coefficients that determine the direction of the velocity polarisation of the fast mode are

$$C_x^f = \frac{c_s^2 k_x k_z - v_A^2 k^2 \cos\theta_m \sin\theta_m}{\sqrt{(c_s^2 k_x k_z - v_A^2 k^2 \cos\theta_m \sin\theta_m)^2 + (\lambda_f - c_s^2 k_x^2 + \omega^2 - v_A^2 k^2 \cos^2\theta_m)^2}}, \tag{90}$$

$$C_z^f = \frac{\lambda_f - c_s^2 k_x^2 + \omega^2 - v_A^2 k^2 \cos^2\theta_m}{\sqrt{(c_s^2 k_x k_z - v_A^2 k^2 \cos\theta_m \sin\theta_m)^2 + (\lambda_f - c_s^2 k_x^2 + \omega^2 - v_A^2 k^2 \cos^2\theta_m)^2}}, \tag{91}$$

$$\vec{\psi}_f = C_x^f \hat{e}_x + C_z^f \hat{e}_z. \tag{92}$$

For the slow mode, the eigenvalue is denoted as λ_s. In this case, we also obtain the same coefficients as for the fast mode (90) and (91), but changing λ_f to λ_s:

$$\vec{\psi}_s = C_x^s \hat{e}_x + C_z^s \hat{e}_z. \tag{93}$$

Let us now consider the limits when $c_s \gg v_A$ or $c_s \ll v_A$, which can tell us which direction each mode prefers to follow as well as characterise each of the modes and distinguish them from each other. Furthermore, it is important to study these limits because plasma $\beta = (2\mu_0 p_0)/B_0^2$, is

[5] To diagonalise a matrix we perform the operation $\det[D - \lambda I] = 0$, where I is the identity matrix and λ are the eigenvalues to be found.

comparable to the ratio c_s^2/v_A^2. In the photosphere, β is typically larger than one ($c_s \gg v_A$). However, in the chromosphere, it is less than one ($c_s \ll v_A$). Starting with equation (83) the frequency of the fast mode when $c_s \gg v_A$ is $\omega \approx kc_s$ and when $c_s \ll v_A$ is $\omega \approx kv_A$, i.e., the phase speed of the fast mode tends to the value which is higher from the sound or the Alfvén speeds. In contrast, the phase speed of the slow mode tends to the lower one, such that when $c_s \gg v_A$ is $\omega \approx kv_A \cos\alpha$ and when $c_s \ll v_A$ is $\omega \approx kc_s \cos\alpha$ (these two approaches are derived in Appendix C where equation (C.14) is for the $c_s \ll v_A$ approximation and (C.13) for $c_s \gg v_A$).

Next, we study the polarisation vector limits, from the approximations shown above, we have that the eigenvalue for the fast mode when $c_s \gg v_A$ is $\lambda_f \approx -\omega^2 + k^2 c_s^2$. Then the coefficients of the polarisation vector (see Appendix C for a detailed computation):

$$C_x^f \approx \sin\phi, \tag{94}$$
$$C_z^f \approx \cos\phi. \tag{95}$$

As it can be seen in Figure 10, ϕ is the angle that $\vec{k}$ forms with respect to the z-axis. In this limit, the fast waves polarisation follows the direction of the acoustic waves, i.e. parallel to the wave vector $\vec{k}$. Now, in the $c_s \ll v_A$ the eigenvalue is $\lambda_f \approx -\omega^2 + k^2 v_A^2$ and the coefficients:

$$C_x^f \approx -\cos\theta_m, \tag{96}$$
$$C_z^f \approx \sin\theta_m. \tag{97}$$

In this case, we have that the direction of the polarisation vector is perpendicular to the magnetic field, since $\vec{B}_0 = \sin\theta_m \hat{x} + \cos\theta_m \hat{z}$ (Figure 10). In summary, we find that when $c_s \gg v_A$ the fast mode has an acoustic wave nature and when $c_s \ll v_A$, a magnetic wave nature.

Now it is the turn of the slow mode. In the $c_s \gg v_A$ limit, the eigenvalue is $\lambda_s \approx -\omega^2 - k^2 v_A^2 \cos^2\alpha$ and the coefficients are

$$C_x^s \approx \cos\phi, \tag{98}$$
$$C_z^s \approx -\sin\phi. \tag{99}$$

Here we get the opposite of what we got in the fast mode case. In this limit, the polarisation vector of the slow mode is perpendicular to the direction of $\vec{k}$. Alternatively, this result was to be expected, given that the fast and slow modes are eigenvalues and their eigenvectors will be orthogonal to each other. When $c_s \ll v_A$ the eigenvalue is $\lambda_s \approx -\omega^2 - k^2 c_s^2 \cos^2\alpha$ and the coefficients are

$$C_x^s \approx \sin\theta_m, \tag{100}$$
$$C_z^s \approx \cos\theta_m. \tag{101}$$

In this case, the slow mode is polarised parallel to the magnetic field and perpendicular to those of the fast mode. In Table 1 we summarise the results obtained for both limits and modes.

	Fast mode	Slow mode
$c_s \gg v_A$	acoustic ($\omega/k \approx c_s$), $\vec{u} \parallel \vec{k}$ (ϕ)	magnetic ($\omega/k \approx v_A \cos\alpha$), $\vec{u} \perp \vec{k}$ (ϕ)
$c_s \ll v_A$	magnetic ($\omega/k \approx v_A$), $\vec{u} \perp \vec{B}_0$ (θ_m)	acoustic ($\omega/k \approx c_s \cos\alpha$), $\vec{u} \parallel \vec{B}_0$ (θ_m)

Table 1: This table shows the speed and polarisation direction of fast and slow modes in the two asymptotic regimes.

In summary, we already have the characteristics and polarisation direction for the fast and slow modes when the magnetic field dominates ($c_s \ll v_A$) or when the pressure forces dominate ($c_s \gg v_A$), i.e. when it is in the chromosphere or photosphere region respectively. However, the speed values can be comparable in a stratified atmosphere. The sound speed remains constant even if we consider again a stratified atmosphere because we also consider it to be isothermal. But the Alfvén speed increases with height, so at some point they are going to be equal, as it can be seen in Figure 11. In the region where the speeds are comparable we recover the coefficients deduced in (90) and (91). In other words, in this region, the modes present both magnetic and acoustic behaviour and they could interact.

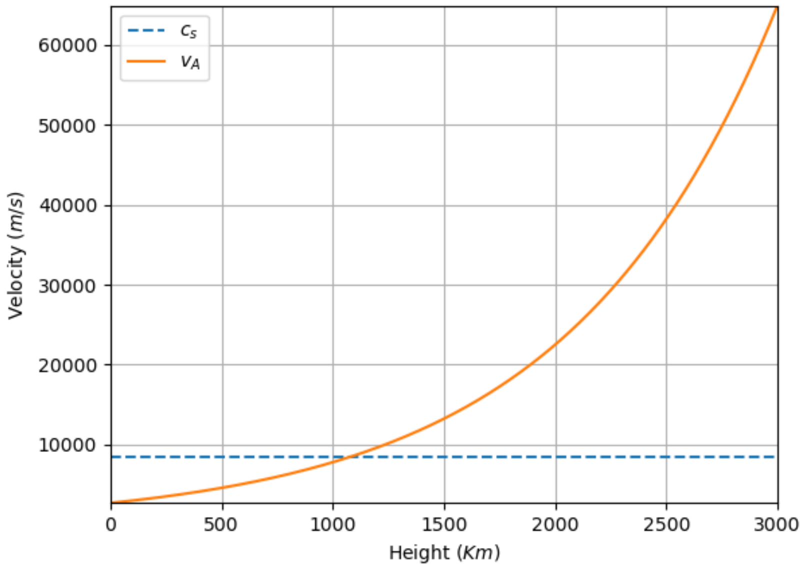

Figure 11: Sound speed (c_s) and Alfvén speed (v_A) profiles of the atmosphere shown in Figure 3 and with $B_0 = 500$ G.

In order to study this region, we present the ray tracing method in the next section, because it allows us to add a stratification in the background quantities. Moreover, by working at high frequencies, we can reuse the terms manipulated in this section, even though they have been described in a homogeneous atmosphere. However, there is still one important detail about magnetoacoustic waves, and that is whether they conserve energy or not.

4.2.2 Energy conservation

As in the case of HD waves (section 3.3.1), we will study the conservation of energy for MHD waves. Part of the work has already been done, so now, including the gravity terms we are going to start with the MHD equations (equations (13)-(17)) presented in the MHD theory section. We now include the gravity terms because, as mentioned above, in the next section we include the stratification of the background quantities. In order to find the energy conservative equation we only need to focus on the magnetic terms, since we have already dealt with the other non-magnetic terms and they are clearly separated from each other. If in the magnetohydrostatic equilibrium, the magnetic field is constant (our case $B_0 = const$), we recover the hydrostatic equilibrium (21). Therefore, only the hydrodynamic background quantities have a dependence on height while the magnetic field is homogeneous.

To find the energy equation in a conservative form we need to take the scalar product with $\vec{u}$ in the momentum equation (14) like we did in section 3.3.1, take the scalar product $\vec{B}'/\mu_0$

with the induction equation (16) and doing some algebra (see Appendix D) we find

$$\frac{\partial}{\partial t}\left(\frac{1}{2}\rho_0 u^2+\frac{p'^2}{2c_s^2\rho_0}+\rho_0 N^2\xi_z^2+\frac{1}{2}\frac{B'^2}{\mu_0}\right)+\nabla\cdot(p'\vec{u})+\frac{1}{\mu_0}\left[\nabla\cdot(\vec{u}(\vec{B}_0\cdot\vec{B}'))-\nabla\cdot(\vec{B}_0(\vec{u}\cdot\vec{B}'))\right]=0. \tag{102}$$

Compared to equation (29) obtained in the HD section, we now have the inclusion of the magnetic energy and following the definition (61) we get

$$e'_{tot}=\frac{1}{2}\rho_0 u^2+\frac{p'^2}{2c_s^2\rho_0}+\rho_0 N^2\xi_z^2+\frac{1}{2}\frac{B'^2}{\mu_0}. \tag{103}$$

In addition, we now have in equation (102) new terms that contribute to the wave energy flux. Equation (102) can be rewritten to take into account the electric field perturbation. This is described in equation (D.3). Furthermore, if we start from equation (D.8) of the appendix, which is previous to the development of the vector product equation (D.9) that leads to the conservation of energy equation (102), we get

$$\frac{\partial}{\partial t}\left(\frac{1}{2}\rho_0 u^2+\frac{p'^2}{2c_s^2\rho_0}+\rho_0 N^2\xi_z^2+\frac{1}{2}\frac{B'^2}{\mu_0}\right)+\nabla\cdot(p'\vec{u})+\frac{1}{\mu_0}\nabla\cdot(\vec{E}'\times\vec{B}')=0. \tag{104}$$

This term $\frac{1}{\mu_0}\vec{E}'\times\vec{B}'$ has the same form as the Poynting vector, $\vec{S}'$ and represents the energy flux of the magnetic terms of the waves.

To check under which conditions magneto-acoustic waves conserve energy, we integrate (104) in a control volume like we did in the case without the magnetic field

$$\frac{d}{dt}\int_{V_{cont}} e'_{tot}dV=-\oint_{\partial V_{cont}} p'\vec{u}\cdot\hat{n}\,dS+\oint_{\partial V_{cont}}\vec{S}'\cdot\hat{n}\,dS. \tag{105}$$

Now, we have two reasons for the total energy in V_{cont} to change. We have already discussed the first one associated with p' in section 3.3.1. The second one associated with the Poynting vector $\vec{S}'$ shows us how much of the energy associated with the electromagnetic terms is leaving the volume. In order to preserve the energy $\vec{u}\cdot\hat{n}=0$ and $\vec{S}'\cdot\hat{n}=0$. The direction of propagation of the electromagnetic field (and the electromagnetic wave) $\vec{S}'$ has to be normal to $\hat{n}$.

In conclusion, if the boundary conditions allow the scalar products to be $\vec{u}\cdot\hat{n}=0$ and $\vec{S}'\cdot\hat{n}=0$, magnetoacoustic waves preserve the energy. This is quite an important result, as it is a necessary condition for the mode conversion formalism that we introduce in the next section (section 5.1), hence the addition of gravity terms.

5 Wave propagation in a weakly inhomogeneous medium

Resumen

El formalismo de MHD ha permitido describir de forma general las características de las ondas magnetoacústicas. Aún así, para obtener una mayor comprensión de su propagación en la atmósfera solar cuando $c_s \sim v_A$, se introducirá en esta sección el formalismo de trazado de rayos presentado en Tracy et al. (2014) para describir estas ondas en un medio débilmente inhomogéneo a frecuencias altas. El formalismo de trazado de rayos aporta una solución aproximada, usando un principio variacional para las ecuaciones del eikonal. Además, se mencionarán las circunstancias en las que dicha aproximación puede fallar. Destacando la de la transformación de modos, ya que como se verá en esta sección, al emplear el formalismo de Tracy et al. (2014) a la matriz de dispersión de las ondas magnetoacústicas se observa como estas pueden sufrir una transformación de modos en la región donde $c_s \sim v_A$.

The MHD formulation has allowed us to know some of the characteristics of the waves that can propagate in the solar atmosphere, as well as the direction of propagation of the magnetoacoustic waves in the two limits discussed in the previous section. Although with this formalism it has been possible to draw many conclusions about these waves, in order to generalise the results we find in homogeneous conditions, we introduce the ray tracing formalism to solve wave equations with inhomogeneous coefficients.

To reduce the algebraic complexity we restrict ourselves to high frequencies, so we can ignore the gravity terms in the perturbation equations even if we keep the gravitational stratification in background quantities. This means that we can use the results obtained for the magnetoacoustic waves, even though these results have been found for a homogeneous medium. Moreover, we can apply the result we obtained in section 4.2.2, because when we derive the energy conservation equation for magnetoacoustic waves we took into account the gravitational stratification confirming its application to the Tracy et al. (2014) formalism. However, these gravitational terms can be included in the study, thus complicating the algebra (Schunker & Cally, 2006). Before introducing the ray tracing method, let us characterise our atmosphere as a weakly inhomogeneous medium. Here, the pressure and density are stratified but their variation scales are much slower than those of the waves. In order to clarify this, we introduce the formal parameter ε which is the ratio of the carrier length scale to the modulation length scale. Therefore, having a small value of this parameter allows us to take the medium as weakly inhomogeneous. In other words, we consider that the characteristic scales of the atmosphere (for instance H), are much larger than wavelength. Now with the medium characterised, let us start our last stage of study, where we introduce the ray tracing formalism presented by Tracy et al. (2014).

5.1 Ray tracing formalism

Ray tracing formalism is a variational method that brings together concepts from geometrical optics such as Fermat's principle, classical Hamiltonian mechanics and physical optics. The wave nature of light is well known, but the concepts of geometrical optics, i.e. ray theory, such as Fermat's principle work quite well in many cases even if they do not take into account the wave nature. Hamilton, in order to provide an answer to how light could be a wave and describe trajectories as a particle (like in ray tracing) constructed a wave field using a new type of ray theory.

First, let us state Fermat's stationary principle, which defines rays as *any path for which the travel time is stationary with respect to small variations*. This means that, if we express the path of light between two points by a functional called the optical path, the actual path of the light will follow an extreme path with respect to this functional. This statement is more complete than the least time principle of Fermat's, as it covers all possible cases and will be the beginning of the basis of the variational method to be used (Tracy et al., 2014).

The ray theory gives us a useful geometrical view of the problem, but in more complex cases such as the plasma forming the solar atmosphere, propagation properties change point to point and, therefore, the rays are no longer straight lines. The Hamilton stationary phase principle extends the concepts of geometrical optics to understand the solutions of a wave equation (because, for instance, in Fermat's theory there is no dispersion relation between the wave frequency and the wavevector since there is no wavevector) in terms of rays. This theory applies to all types of waves and it assumes that the wave field is in the form of a rapid variation characterized by

$$\vec{\psi} = Ae^{i\theta}e^{i\varphi}\hat{e}, \tag{106}$$

where the phase θ varies rapidly, A is a real amplitude that varies slowly, φ is the polarisation phase and $\hat{e}$ the unit polarisation vector. Equation (106) is the solution of the wave equation in eikonal form. Eikonal solutions have that θ and A are real functions, which allows us to define the following relations:

$$\vec{k} \equiv \nabla\theta, \; \omega \equiv -\frac{\partial\theta}{\partial t}. \tag{107}$$

Therefore, we reduced the problem to eikonal problems. We restrict solutions to eikonal approximations for the wave equation that describes the propagation of waves in which the phase varies rapidly while the amplitude varies slowly. In Hamilton's theory, the phase function plays an important role, since it could be written as the integral of some function along one-dimensional paths (these will become the rays). Therefore, the phase of the eikonal plays the same role as the Hamiltonian. We have already described the shape of the approximations to the solutions of the wave equation and the main characteristics. The last step is to determine the path that the ray follows, which is described by Hamilton's equations.

We have already presented the general idea of the ray tracing method using Hamilton's equations. Now we will describe the dispersion function concept in order to apply this methodology step by step. Inserting the eikonal *ansatz* (106) in a wave equation written as follows

$$\bar{\bar{\mathcal{D}}}(-i\nabla, i\partial t)\vec{\psi}(\vec{r}, t) = 0, \tag{108}$$

we arrive at the condition

$$\bar{\bar{\mathcal{D}}}(k, \omega) = 0, \tag{109}$$

where $\mathcal{D}(k, \omega)$ is the dispersion function and the curves that fulfil the last condition are the dispersion curves.

Then, we follow Tracy et al. (2014) and we use Hermitian matrix to ensure that the dispersion functions and rays are real. The motivation is that we want the ray to describe the wave propagation. For example, in section 3.1, we found that below the cut-off frequency, the waves became evanescent, this happened when we obtained purely imaginary results. And we want that our rays follow a "real" path. This is the dispersion matrix whose eigenvalues are real and we assume that they are nondegenerate, so the associated eigenvectors are orthogonal. Now, we can introduce the Hamilton variational principle described previously (we insert the eikonal *ansatz* (106)). The dispersion function that arises is one of the eigenvalues of the dispersion matrix, restricted to zero in phase space (has to fulfil condition (109) to be a Hamiltonian ray) and the polarisation is its associated eigenvector. This is analogous to how it was developed in the previous section of magnetoacoustic waves (section 4.2.1). Besides we adopt that they form an orthonormal basis

$$\hat{e}^{\dagger}_{\beta}(\vec{r}, \vec{k}) \cdot \hat{e}_{\alpha}(\vec{r}, \vec{k}) = \delta_{\beta\alpha},$$

where β and α denote different eigenvalues.

The last step is to use Hamilton's equations to describe the path that the ray follows. This reduces the system of partial differential equations that we had to a system of ordinary differential equations. In the Hamilton equations, D_α is the dispersion relation for a specific eigenvalue, plays the role of the Hamiltonian and therefore, the phase space is filled with trajectories that are solutions of the equations, but only the ones that fulfil $D_\alpha(\vec{r}, \vec{k} = \nabla\theta) = 0$ are the Hamiltonian rays. Nevertheless, we can also use the determinant of the matrix symbol as the Hamiltonian ray $\mathcal{D} = \det(D)$, since it can provide us with certain advantages, like avoiding the diagonalisation of the matrix or the information that the determinant contains of the eigenvalues, which becomes important if, for example, two eigenvalues are close to zero. The use of the determinant as a dispersion matrix leads to the same rays, but with a change in the parameterisation in the Hamilton equations, since the determinant is the product of the eigenvalues and the rays are restricted to $\mathcal{D} = 0$. Which a dispersion function defined

$\mathcal{D} = \det(D)$, the ray paths follow:

$$\frac{d\vec{r}}{d\sigma} = \nabla_{\vec{k}}(\mathcal{D}),\ \frac{d\vec{k}}{d\sigma} = -\nabla_{\vec{r}}(\mathcal{D}),\ \frac{dt}{d\sigma} = -\frac{\partial \mathcal{D}}{\partial \omega},\ \frac{d\omega}{d\sigma} = \frac{\partial \mathcal{D}}{\partial t}, \tag{110}$$

where σ is the variable that parametrises the path of the ray and only depends on $\mathcal{D}$. In our specific case, we have seen that the atmosphere is stratified in the vertical component $\hat{z}$. Therefore, $\mathcal{D}$ will be independent of the horizontal component x, so k_x will remain constant along the ray, and if $\mathcal{D}$ is independent of t, ω it will also remain constant.

There are circumstances when the ray tracing method fails: caustics, tunneling and mode conversion. Caustics are associated with local singularities that can arise when the rays are projected from the ray phase space to the x space. This leads to a loss of good behaviour of the eikonal phase, which results in nonphysical predictions. However, in this case, it is always possible to find a local representation in which the eikonal approximation is valid. In contrast, in tunneling and mode conversion there is no representation where the eikonal approximation is valid. Tunneling concerns only one eigenvalue of the dispersion matrix and mode conversion two. For example, tunneling can occur because a ray that encounters a barrier it cannot overcome energetically splits into two rays, one reflected and the other transmitted. Still, such a ray maintains the same properties. On the other hand, in mode conversion, there are two modes with different characteristics that exchange energy. A possible example of this phenomenon taking place on Earth is found in the Gulf of Guinea, where there are coastally trapped waves propagating westward that may interact with and transform into equatorially trapped waves propagating eastward (Tracy et al., 2014).

Here, we focus on the mode conversion and the matched asymptotic methods presented in Tracy et al. (2014) to overcome the failure in the ray theory to describe it. Although the eikonal approximation is not working in this region we continue to insist on applying ray tracing, since we can use the fact that the dispersion matrix does not depend on the eikonality, so it can be Taylor expanded about any point. The conversion matching provides us with a simple, but general formulation of the problem, so let us begin with this formulation.

Our dispersion matrix has two eigenvalues associated with the dispersion curves $D_\alpha(x,k) = 0$ and $D_\beta(x,k) = 0$, which present avoided crossings where the two eigenvalues in this neighbourhood are near zero. The failure of the ray tracing method is the assumption that the modes are distinguishable at this point. Far from the conversion point the eikonal assumption is valid and it can be associated with a ray. Therefore, the approach consists in using the ray asymptotes far from the conversion point to interpolate the incoming and outgoing rays of this point. The goal is to eliminate the avoided crossing behaviour and reconnect the paths after going through the conversion point. With a self-adjoint operator, we have the associated variational principle for the local wave equation in one dimension

$$\mathcal{A}(\Psi) = \int dx\, \vec{\Psi}^\dagger(x) \cdot D_{n\times n}(x, -i\partial) \cdot \vec{\Psi}(x),$$

and we can insert the following *ansatz* into the variational principle

$$\vec{\Psi}(x) = \Psi_A(x)\hat{e}_A + \Psi_B(x)\hat{e}_B,$$

where $\vec{\Psi_A}(x)$ and $\vec{\Psi_B}(x)$ are not eikonal form and they are n-dimensional vectors. Following the general mode conversion theory of Tracy et al. (2014) is possible to put the dispersion matrix into a normal form, which is the simplest representation of the problem using the geometry of the incoming and outgoing rays. Therefore, the dispersion matrix is

$$D(x,k) = \begin{pmatrix} D_A & \tilde{\eta} \\ \tilde{\eta}^* & D_B \end{pmatrix}. \tag{111}$$

These two new polarisations that go smoothly to the conversion point provide us with an approximation of how the eigenvalues would behave at the conversion point. Here, the two dispersion surfaces ($D_A = 0$, $D_B = 0$) would cross and the associated polarisations would change smoothly throughout the conversion region as shown in Figure 12.

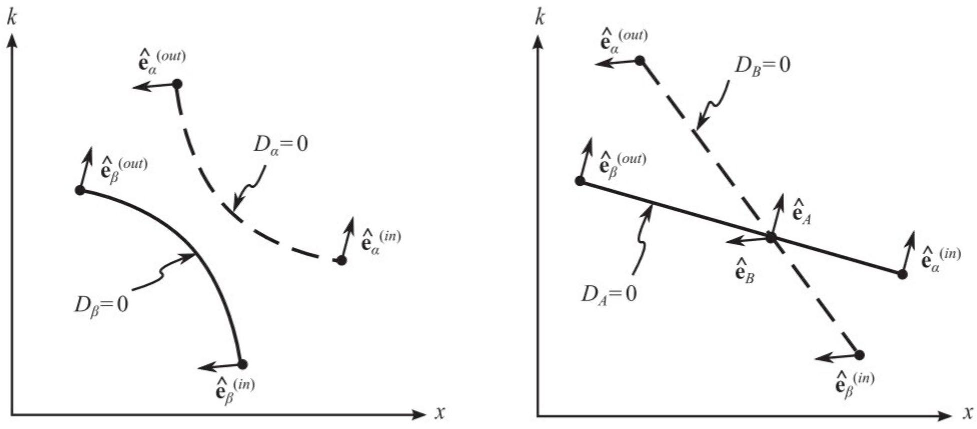

Figure 12: On the left, a representation of the dispersion curves $D_\alpha = 0$ and $D_\beta = 0$ that illustrates the behaviour of the rays near the conversion point, the called avoided crossing. On the right, a representation of the same region but with the dispersion curves $D_A = 0$, $D_B = 0$ associated with the new polarisation vectors which, far from the conversion region, are again those associated with the eikonal (Tracy et al., 2014).

Note that the mode conversion depends on the dispersion matrix and not just the determinant, since this leads to the fact that an incoming ray connects to its converted ray, but not its transmitted ray. In the dispersion matrix (111) $\tilde{\eta}$, the coupling term, is small compare to D_A and D_B where the eikonal approximation is valid $\mathcal{D} = D_A D_B - |\tilde{\eta}|^2 \approx D_A D_B$, therefore the matrix is diagonal and $\mathcal{D} = 0$ where D_A and D_B represents the eigenvalues decoupled. However, near the conversion point, the value of $\tilde{\eta}$ becomes comparable and quantifies the mode transmission. Then the general theory requires performing a linear canonical transformation and a rescaling. That done, the coupling parameter is

$$\eta = \frac{\tilde{\eta}}{|\{D_A, D_B\}|^{1/2}}, \tag{112}$$

where $\{D_A, D_B\}$ is the Poisson bracket[6] of the uncoupled dispersion functions. Finally, we introduce the transmission and conversion coefficients that determine the shape of the outgoing rays

$$\tau = e^{-\pi|\eta|^2},\ \kappa = -\frac{\sqrt{2\pi\tau}}{\eta\Gamma(-i|\eta|^2)}, \tag{113}$$

where τ is the transmission coefficient and κ the conversion coefficient (Tracy et al., 2014). In the conversion coefficient Γ is the Gamma function, which fulfills the expression $|\Gamma(iy)|^2 = \frac{\pi}{\sinh \pi y}$ where y is real (Abramowitz et al. (1988), equation 6.1.29). The convention for κ is that when the converted rays are moving to the right of the incoming ray the conversion is κ, but if it is moving to the left is $-\kappa^*$. Therefore, the amount of energy transmitted is $T = \tau^2$ and the amount of energy converted $C = |\kappa|^2$ fulfilling that $T + C = 1$, so the energy is conserved.

[6]The Poisson bracket is defined as: $\{D_A, D_B\} = \frac{\partial D_A}{\partial x}\frac{\partial D_B}{\partial k} - \frac{\partial D_B}{\partial x}\frac{\partial D_A}{\partial k}$

5.2 Application of mode conversion formalism

Let us put the ray tracing formalism into practice. We have our self-adjoint matrix (88) derived in MHD from the magnetoacoustic wave section. With a stratified atmosphere in the vertical direction (z), uniform in the horizontal direction (x) and with the possibility to fix a certain frequency, therefore, the dispersion function is independent of t, and k_x remains constant along a ray. When we diagonalised the dispersion matrix (88), we obtained the fast and slow modes and we studied the asymptotic behaviour of these modes in the limits $c_s \gg v_A$, $c_s \ll v_A$. In other words, we studied their behaviour in the photosphere ($c_s \gg v_A$) and the chromosphere ($c_s \ll v_A$). Now, we focus on the natural modes, i.e. the asymptotic normal modes that refer to the nature of the restoring force of the wave (acoustic and magnetic waves) instead of fast and slow modes. We find that when we are not in the regions where these limits dominate ($c_s \approx v_A$), both modes are coupled. As seen in the theoretical part of the ray tracing method, the eikonal approximation can be applied to these limits since the eigenvalues are not degenerated. Although, it remains to be seen whether it is possible to do so in the intermediate region.

Following the method shown for the mode conversion we need a smooth path that links these regions. Therefore, our *ad hoc* matrix will rotate the system to the acoustic waves direction when $c_s \gg v_A$ and to the direction of the magnetic field when $c_s \ll v_A$. This will cause our reference system to follow smoothly the acoustic mode direction. Usually, we obtain a dispersion matrix in a certain base and then we find the eigenvectors. But here we start "creating" the eigenvectors and then we look for the eigenvalues. In this way, we begin defining the *ad hoc* matrix for acoustic mode. Since the eigenvectors are orthonormal, the magnetic eigenvectors can be obtained by calculating the perpendicular vector to the acoustic eigenvalue. As previously mentioned we are going to follow the polarisation direction of acoustic waves by our *ad hoc* rotation matrix. This is done taking into account the behaviour at the limits ($c_s \gg v_A$, $c_s \ll v_A$) which is detailed in Table 1. Therefore, our *ad hoc* matrix for the acoustic mode is

$$R_{ac} = \frac{1}{\sqrt{(c_s^2 \sin\phi + v_A^2 \sin\theta_m)^2 + (c_s^2 \cos\phi + v_A^2 \cos\theta_m)^2}}(c_s^2 R(\phi) + v_A^2 R(\theta_m)), \tag{114}$$

where

$$R(\phi) = \begin{pmatrix} \sin\phi & \cos\phi \\ \cos\phi & -\sin\phi \end{pmatrix} \tag{115}$$

and $R(\theta_m)$ is the rotation matrix (86) introduced when we defined $k_\parallel$ and $k_\perp$. Matrix $R(\phi)$ rotates the frame of reference to the direction of $\vec{k}$, matrix $R(\theta_m)$ to the direction of the magnetic field. And matrix R_{ac} is the combination of both such that, depending on which speed dominates it rotates to one system, the other or a combination of both. This rotation matrix allows the change to acoustic basis but it is still necessary to transform the dispersion matrix D that we obtained in MHD formalism (88). Since it rotates the system in the vector basis of the vectors $\hat{x}$ and $\hat{z}$ and not in the basis of the new polarisation vectors $\hat{e}_{ax}$, $\hat{e}_{az}$, where the a subindex denotes acoustic mode.

$$D' = R^{-1} D R. \tag{116}$$

Matrix D' is the dispersion matrix in the acoustic basis and it has the following elements:

$$\begin{aligned} D'_{11} = {}& -c_s^2 \left[k^4(v_A^4 + v_A^2 c_s^2 + 2c_s^4)\right] - 4v_A^2 c_s^4 k^3 k_\parallel + 2k\omega^2 \left[(v_A^4 + c_s^4)k + 2v_A^2 c_s^2 k_\parallel\right] \\ & + v_A^2 c_s^2 (v_A^2 - c_s^2)(k_x^4 - k_z^4)\cos 2\theta - 2v_A^2 c_s^2 (v_A^2 - c_s^2) k^2 k_x k_z \sin 2\theta, \end{aligned} \tag{117}$$

$$\begin{aligned} D'_{22} = {}& -v_A^2 \left[k^4(2v_A^4 + v_A^2 c_s^2 + c_s^4)\right] - 4v_A^4 c_s^2 k^3 k_\parallel + 2k\omega^2 \left[(v_A^4 + c_s^4)k + 2v_A^2 c_s^2 k_\parallel\right] \\ & - v_A^2 c_s^2 (v_A^2 - c_s^2)(k_x^4 - k_z^4)\cos 2\theta - 2v_A^2 c_s^2 (v_A^2 - c_s^2) k^2 k_x k_z \sin 2\theta, \end{aligned} \tag{118}$$

$$D'_{12} = D'_{21} = -2v_A^2 c_s^2 (v_A^2 + c_s^2) k^2 (k + k_\parallel) k_\perp, \tag{119}$$

where $D'_{11} = 0$ and $D'_{22} = 0$ represent the acoustic and magnetic asymptotic eigenvalues, respectively. Let us see whether these curves intersect at some point, i.e. if there exists an ordered pair (z, k_z), such that $D'_{11} = D'_{22} = 0$ and the eikonality breaks.

$$D'_{11} = D'_{22},$$

$$2\frac{c_s^4}{v_A^2} - 2\frac{v_A^4}{c_s^2} = 4\cos\alpha(c_s^2 - v_A^2) + 2v_A^2 c_s^2 (v_A^2 - c_s^2)(k_x^4 - k_z^4)\cos 2\theta \frac{1}{k^4}.$$

So, D'_{11} and D'_{22} intersect when $c_s = v_A$, with this pair (z, k_z) being our conversion points. This occurs in the equipartition zone (where the speeds are comparable) which separates the photosphere and chromosphere as we have discussed in section 4.2.1 with the help of Figure 11 and the study of the limits.

The non-diagonal elements of our matrix represent the coupling terms and how much coupled are the modes. Due to the choice of our *ad hoc* matrix, we have that far from the conversion points the coupling terms tend to zero. Consequently, $\det(D') = D'_{11}D'_{22} - D'_{12}D'_{21} \approx D'_{11}D'_{22}$. The two modes are decoupled in these limits. As we have a stratified atmosphere in the vertical component, z-axis, the horizontal components will remain constant, so the approximate value of k_z when the mode conversion takes place $(c_s = v_A)$ is

$$-c_s^2(4k^4c_s^4) - 4c_s^6k^3k_\parallel + 2k\omega^2(2c_s^4k + 2c_s^4k_\parallel) = 0$$
$$4c_s^4k(-k^3c_s^2 - k^3c_s^2\cos\alpha + \omega^2k + \omega^2k\cos\alpha) = 0$$
$$-k^2c_s^2(1+\cos\alpha) + \omega^2(1+\cos\alpha) = 0$$

$$k^2 = \frac{\omega^2}{c_s^2} \Rightarrow k_z = \sqrt{\frac{\omega^2}{c_s^2} - k_x^2}. \tag{120}$$

The value of k_z can be obtained by taking into account that the speed of sound is constant by being in an isothermal atmosphere. On the other hand, by fixing the value of k_x, the reflection condition $(k_z = 0)$ occurring in the chromosphere can be obtained. To do this, we return to the dispersion equation (83) and the condition $v_A \gg c_s$, because it occurs at the chromosphere. We get

$$\omega^2 \approx k^2 v_A^2,$$

$$k_z = \sqrt{\frac{\omega^2}{v_A^2} - k_x^2} \Rightarrow \frac{\omega}{v_A} < k_x. \tag{121}$$

So, upward propagating rays are reflected when this condition is fulfilled; a ray propagates when its eigenvalue is real in the ray tracing formalism; and when $\omega/v_A < k_x$, k_z becomes evanescent and its solution is no longer real. Therefore, a way propagating upwards $(k_z > 0)$, at this height (when $k_z = 0$, i.e $\omega/v_A = k_x$) it is going to be reflected and it propagates downwards $(k_z < 0)$ to keep moving in the "real" line.

As explained in the presentation of the ray tracing formalism, in the case of mode conversion it is not possible to apply the eikonal approximation. But we can use our matrix, as it does not depend on the eikonality of the wave field as well as the Weyl symbols, which will allow us to construct local wave equations. This uses the geometry of the incoming and outgoing rays that pass through the conversion point. In other words, it is possible to apply the method followed by Tracy et al. (2014) and explained in section 5.1 since our magnetoacoustic waves conserve energy like in this method (section 4.2.2). In this work, we will not go into this, i.e. calculating the transmission, conversion coefficients and making the asymptotic matching with the outgoing and incoming rays. But we will make a qualitative discussion of these results. For this purpose, in the next section, we show the crossing of the magnetic and acoustic asymptotic curves with the full dispersion curves $\mathcal{D} = 0$. This is the relation (83) in the magnetoacoustic waves section. But now we are going to solve it as a function of k_z since it is the value that changes due to stratification. Note that in this expression α and k depend on k_z. Therefore the dispersion relation is

$$k_z^2 + k_x^2 - \omega^2 \left[\frac{(c_s^2 + v_A^2)}{2} \pm \frac{\sqrt{(c_s^2 + v_A^2)^2 - 4v_A^2 c_s^2 \cos^2\alpha}}{2} \right]^{-1} = 0, \tag{122}$$

$$\cos\alpha = \frac{k_\parallel}{k} = \frac{k_x \sin\theta_m + k_z \cos\theta_m}{\sqrt{k_x^2 + k_z^2}}. \tag{123}$$

In the next section, we discuss the results for different fixed values of the frequency and inclination of the magnetic field (θ_m).

5.3 Discussion of results

Now, we know how to describe what happens to the magnetoacoustic waves inside the equipartition region (the frontier of the photosphere-chromosphere, where $c_s \approx v_A$) and how the mode conversion from fast-acoustic to fast-magnetic or slow-magnetic to slow-acoustic occurs. This may also happen in regions where there is a sudden change of dominant force, such as an acoustic wave propagating through the photosphere and approaching a sunspot. In summary, we already know that the solar atmosphere can provide the necessary conditions for this phenomenon to take place, but let us take a qualitative look at some of its characteristics from a discussion of the following results shown in Figure 13, where k_z has been represented as a function of the height z for different magnetic angles (θ_m) and frequencies.

The first thing to note in Figure 13 is that the dispersion curves are asymmetrical, i.e. a wave propagating upwards does not have the same behaviour as one propagating downwards. Therefore, it will not transmit or convert the same energy, even though the energy must be conserved in any case. On the one hand, the figures represent quite well the changes in the dispersion curves due to the values of the main parameters affecting the mode conversion. For instance, at lower frequencies, the branches tend to get closer to the conversion points causing them to become more like the $D_{11} = 0$ (acoustic) and $D_{22} = 0$ (magnetic) curves in this region and not only when they asymptotically tend towards the eikonal approach. This favours transmission (fast-acoustic to slow-acoustic or slow-magnetic to fast-magnetic) against conversion, because the ray will tend to follow the D_{11} and D_{22} curves. However, as it can be seen from the figures, the change in the inclination of the magnetic field (θ_m) has a larger effect than the frequency. Nevertheless, the change in magnetic field inclination is not important by itself. In fact, it is the angle of attack (α) to which it is related by $\alpha = \phi - \theta_m$ that is important (Figure 9). This is because we consider waves that propagate vertically $\vec{k} \parallel \hat{z}$.

However, let us go back to what Figure 13 shows about the angle θ_m: at high values, there is more amount of energy associated with the conversion. Therefore, the larger the angle, the larger gap between the curves associated with our approach in the conversion region that indicate the transmission. It is as if the direction of the magnetic field acts as a filter for the amount of energy input to the transmission or conversion of modes. To clarify this concept, we present in Figure 14 different snapshots of simulations showing how the mode conversion occurs when crossing the region where $c_s = v_A$ for different angles. These simulations represent the longitudinal velocity, i.e. the component along the direction of propagation $\vec{k}$ when $c_s \gg v_A$ (which we take $\vec{k} \parallel \hat{z}$) and when $c_s \ll v_A$ is the component along the magnetic field. Therefore, this velocity component represents the acoustic waves, those in which we have made the change of base by our *ad hoc* matrix. These simulations use a Gaussian pulse as a periodic driver in the

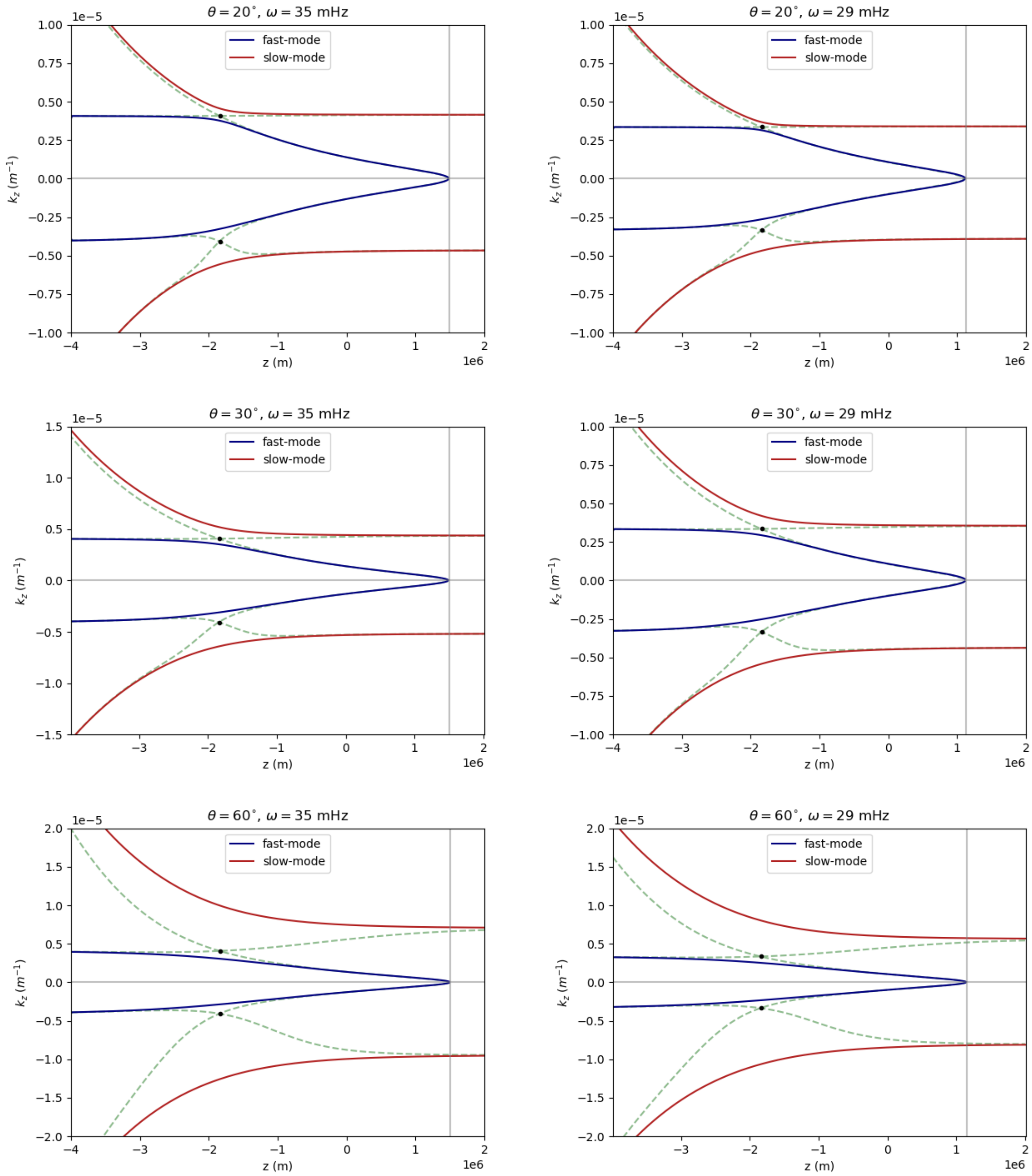

Figure 13: Dispersion diagrams for three different $\theta_m = 20°, 30°, 60°$. The left column corresponds to $\omega = 35$ mHz, $k_x = 0.7$ $\mathrm{M}m^{-1}$, $B_0 = 500$G and the right column to $\omega = 29$ mHz, $k_x = 0.7$ $\mathrm{M}m^{-1}$, $B_0 = 500$G. The background quantities are those of our atmosphere, i.e., those of Figure 3. The dashed curves are the acoustic $D'_{11} = 0$, magnetic $D'_{22} = 0$ and the black points at which they cross, the conversion points $c_s = v_A$. Finally, the grey lines indicate where the reflection of the fast mode waves occurs.

bottom boundary and the atmosphere model employed is the same as the one we have already used and presented in this work (Figure 3, Figure 11).

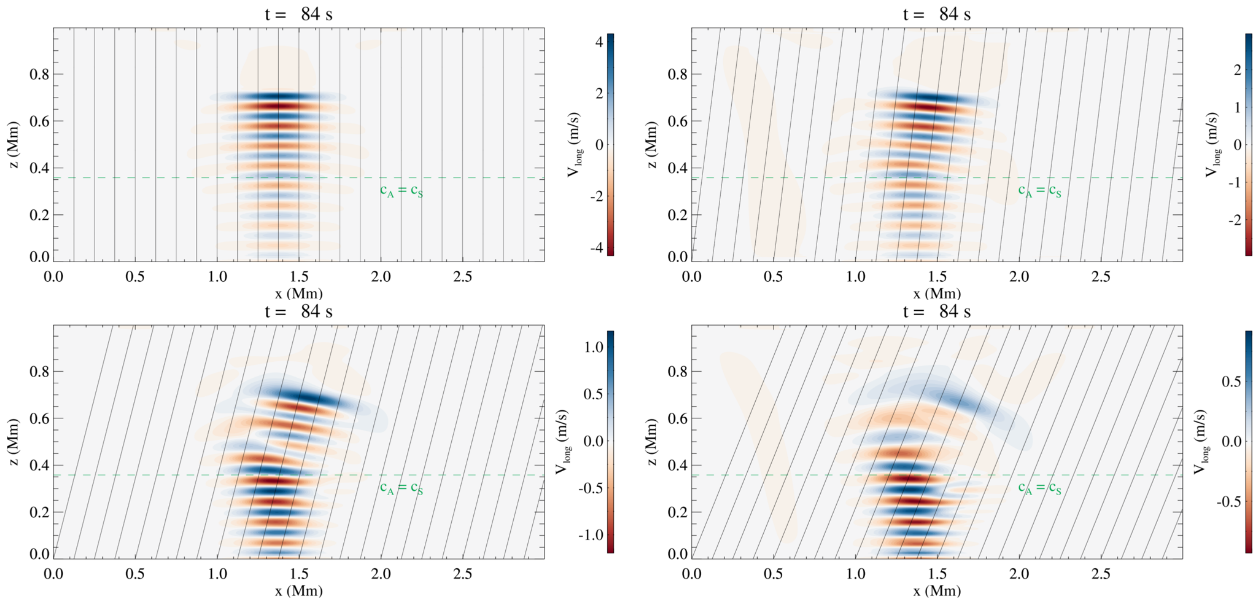

Figure 14: The snapshots represent the longitudinal component of the velocity, where the black lines at the background represent the magnetic field lines and the green horizontal line the height at which the velocities $c_s = v_A$. The first panel corresponds to $\theta_m = 0°$, the second one to $\theta_m = 10°$, the third one to $\theta_m = 20°$ and the last one to $\theta_m = 30°$ ($\omega = 600$mHz).

These figures represent quite well what was discussed previously, since as it can be seen in the two panels of the first row (angles $\theta_m = 0°$ and $\theta_m = 10°$) small angles favour transmission. Below the horizontal line, which indicates $c_s = v_A$, the waves propagate vertically and once they pass this line they tend to follow the magnetic field lines. (fast-acoustic to slow-acoustic transmission occurs). But as the angle increases, mode transmission decreases in favour of conversion as can be seen in the two panels of the last row (angles $\theta_m = 20°$ and $\theta_m = 30°$). These panels show how the polarisation velocity no longer tends to follow the magnetic field lines clearly, decreasing the values of the longitudinal component of the velocity and consequently decreasing the mode transmission. However, we remember that the mode conversion is given by α and that this discussion about that high θ_m favours mode conversion, is associated with α values, but due to our choice of vertical propagation these angles coincide.

This study will remain as a qualitative analysis of the mode conversion phenomenon. Even so, with what we have obtained, it would be possible after performing the asymptotic matching with the incoming and outgoing eikonal waves, to obtain the transmission and conversion coefficients. For this purpose, the coupling parameter (112) at the conversion point has to be evaluated. This is done in Schunker & Cally (2006) and Cally & Gómez-Míguez (2023). Here, we will not go too much into this part, since the corresponding mathematical development has not been carried out, but we will name a parameter that appears in η and therefore, in the transmission coefficient (113). This parameter is called h_s and represents the distance traversed by the oblique ray crossing the horizontal slab of thickness h, where h is the scale height of the conversion layer and when the magnetic field is uniform, is the pressure scale height.

The transmission coefficient shown by Schunker & Cally (2006) (in their article they also take into account the Brunt-Väisälä frequency and the cut-off frequency) is

$$T = \exp(-\pi K h_s \sin^2 \alpha)_{v_A = c_s}, \tag{124}$$

where h_s is the parameter mentioned previously and K is k in the conversion point, i.e $K = \omega/c_s$. If we fix α we can draw the following conclusions attending the term Kh_s: when $Kh_s \gg 1$ the transmission will tend to zero and when $Kh_s \ll 1$ there will be a high transmission from fast-acoustic to slow-acoustic. This is the same as what we discussed before about the frequencies (because $K = \omega/c_s$). Let us discuss this from the point of view of the ray by the wavelength description. The wavelength describes the distance from crest to crest of the wave, at this distance, the properties of the wave cannot change. Therefore, at low frequencies, we have long wavelengths, which makes it difficult to change his behaviour (the mode conversion). In contrast, at high frequencies, the wavelength is small, which facilitates mode conversion. To see this from the point of view of the ray, let us go back to Figure 13. The rays at low frequencies will have to make steeper bends in order to change their properties, due to the long wavelength (i.e. it will have to make a sharp turn to stay on the fast or slow mode curve). Therefore, it is easier for them to follow a straight line following the D_{11} or D_{22} curves while maintaining their properties (transmission). And at higher frequencies, these curves are smoother (because the wavelength is smaller), allowing the rays to easily stay on the curve and change their properties.

Regarding the dependence of T on α, we come to the same conclusions as previously that at smaller angle, higher the transmission. Therefore, for $\alpha = 0$ there is a total transmission. This variation of the transmission coefficient with attack angle is shown in Figure 15.

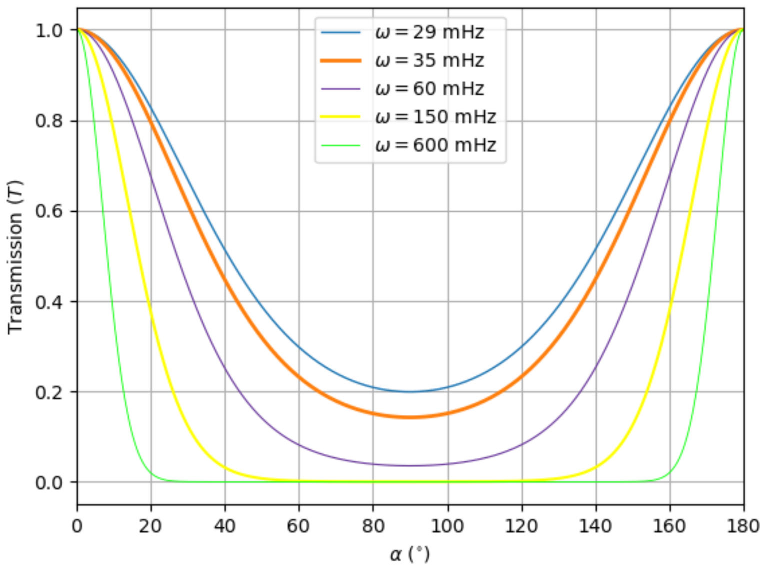

Figure 15: The transmission coefficient (T) as a function of the attack angle (α) for several frequencies. The curves for frequencies used in Figure 13 are $\omega = 29$ mHz (blue line) and $\omega = 35$ mHz (orange line), while the one used in Figure 14 is $\omega = 600$ mHZ (green line).

This figure shows quite clearly the results discussed above: at small angles and low frequencies the transmission coefficient increases and consequently, the amount of energy destinated to transmission (fast-acoustic to slow-acoustic or slow-magnetic to fast-magnetic). Figure 15 can be linked to the simulation snapshots for a better understanding of both. First, these animations are at 600mHz which corresponds to the green curve of Figure 15, showing that due to the high frequencies, transmission is practically zero at angles greater than 20°. This corresponds to what was observed in Figure 14, since the value of the longitudinal component of the velocity when the angle is 30° is about 0.5 m/s at most. On the contrary, when the angle is 0°, the transmission is maximum and there is no mode conversion and the value of the velocity is about 4 m/s.

6 Conclusions

Resumen

Atendiendo a los factores que hemos considerado (gravedad y campo magnético hemos estudiado algunas de las ondas que se podrían propagar en el Sol: las acústico-gravitatorias, acústicas, magnetoacústicas y las ondas de Alfvén. Se pudo comprobar que a altas frecuencias se pueden describir las ecuaciones linearizadas sin tener en cuenta los términos gravitatorios, ya que los modos g se propagan a bajas frecuencias. Al igual que pudimos continuar el estudio sin tener en cuenta las ondas acústico-gravitatorias, ignoramos las ondas Alfvén, puesto que pasamos de un estudio 3D a uno 2D. También obtuvimos que las ondas magnetoacústicas presentan dos modos con comportamientos contrarios en los límites $c_s \gg v_A$ *(fotosfera) y* $c_s \ll v_A$ *(cromosfera). Esto fue descrito en una atmósfera homogénea, pero llegamos al razonamiento de que si estuviésemos en una inhomogénea habría una región en la que estas velocidades son comparables (región de equipartición) y dichos modos podrían interactuar. La consideración de trabajar a altas frecuencias nos permitió trasladar los términos obtenidos en un medio homogéneo a uno débilmente inhomogéneo permitiendo describir las ondas magnetoacústicas usando el formalismo de trazado de rayos. Esto último nos permitió llegar al resultado más importante de este trabajo: cuando se igualan la velocidad de Alfvén y la del sonido* ($c_s = v_A$) *se produce una transformación de modos en la cual se transfiere energía de un modo a otro.*

In this work, we found several results and conclusions on the way to understanding what happens to magnetoacoustic waves propagating from the photosphere to the chromosphere. One of these was that the acoustic-gravity waves have two important frequencies (the Brunt-Väisälä frequency and the cut-off frequency) caused by the gravitational stratification of the atmosphere. These frequencies characterise the acoustic-gravity waves and their effects can be excluded if the gravity terms are not included in the perturbation equations, so high frequencies were used. In addition, we obtained that the Alfvén waves are polarised in the perpendicular direction of the plane defined by the magnetic field and the wavevector. This allowed the problem to be further simplified by moving from a 3D to a 2D configuration, making Alfvén waves unrelated to our study.

Then, studying magnetoacoustic waves in a homogeneous medium, we find the behaviour of the fast and slow modes in the photosphere and chromosphere:

- In the photosphere ($c_s \gg v_A$), the fast mode presents an acoustic nature, i.e the phase velocity is the sound speed c_s and it is polarised in the direction of $\vec{k}$. The slow mode presents a magnetic nature and its polarisation is perpendicular to $\vec{k}$.
- In the chromosphere ($c_s \ll v_A$), the fast mode is magnetic and its polarisation is perpendicular to $\vec{B}_0$. And the slow mode is acoustic and it is polarised in the direction of $\vec{B}_0$.

We have also discussed that in the equipartition region, where the sound speed and Alfvén speed are of the same order, the two modes can interact, which could lead to mode conversion between these modes. To check this, we extended the study to a weakly inhomogeneous atmosphere and applied the ray tracing formalism presented in section 5.1 to the previous results. We created an *ad hoc* matching so that we could rotate our dispersion matrix to the acoustic base. This enabled us to observe the connectivity between the fast and slow modes by the crossing of the acoustic $D_{11} = 0$ and magnetic $D_{22} = 0$ curves, confirming the premise that when the Alfvén and sound speeds are equal, mode conversion occurs. In our case, this phenomenon takes place at the photosphere-chromosphere boundary. From this outcome, it could be observed qualitatively that mode conversion depends on several parameters such as:

- The attack angle α: at high α values the gap between the fast and slow branches becomes wider and favours mode conversion against transmission. At small α there is more transmission, as shown in Figure 15 and equation (124). This angle acts as a filter for the amount of energy input to the transmission mode and consequently mode conversion.
- The frequency that is related to the wavelength (are inversely proportional) appears in the transmission coefficient (124) by $Kh_s = (\omega/c_s)h_s$. This produces that at high frequencies (small λ), $Kh_s \gg 1$ conversion is near-total.

The ray theory has been quite useful in interpreting the results and understanding what happens in the conversion region. In conclusion, it tells us what happens between the two limits ($c_s \gg v_A, c_s \ll v_A$) for fast-acoustic to fast-magnetic or slow-magnetic to slow-acoustic through an acoustic-magnetic conversion and how depending on the conditions, the amount of energy associated with the transmission or conversion is distributed in such a way that it is conserved. This characterisation might be important in studies of chromospheric heating because the mechanisms for energy release depend on each mode.

Appendix A: Acoustic-gravity waves, dispersion relation

To calculate the wave equation for the velocity (50), it is necessary to calculate the temporal derivative of the motion equation (48) and then the gradient of the energy equation (49):

$$\rho_0 \frac{\partial^2 \vec{u}}{\partial t^2} = -\frac{\partial}{\partial t}\nabla p' - g\frac{\partial \rho'}{\partial t}\hat{z}, \quad \text{(A.1)}$$

$$\frac{\partial}{\partial t}\nabla p' = \hat{z}\gamma\rho_0 g\nabla\cdot\vec{u} - \gamma p_0\nabla(\nabla\cdot\vec{u}) + \hat{z}gu_z\frac{d\rho_0}{dz} + \rho_0 g\nabla u_z \quad \text{(A.2)}$$

$$\Rightarrow \rho_0\frac{\partial^2\vec{u}}{\partial t^2} = -\hat{z}\gamma\rho_0 g\nabla\cdot\vec{u} + \gamma p_0\nabla(\nabla\cdot\vec{u}) - \hat{z}gu_z\frac{d\rho_0}{dz} - \rho_0 g\nabla u_z + \hat{z}g\rho_0\nabla\cdot\vec{u} + \hat{z}gu_z\frac{d\rho_0}{dz}. \quad \text{(A.3)}$$

Finally, we arrive at the wave equation (50):

$$\frac{\partial^2\vec{u}}{\partial t^2} = c_{s0}^2\nabla(\nabla\cdot\vec{u}) - \hat{z}(\gamma-1)g\nabla\cdot\vec{u} - g\nabla u_z. \quad \text{(A.4)}$$

The solution is given by (51). And to obtain the dispersion relation (52) we start with the following relations:

$$\frac{\partial^2\vec{u}}{\partial t^2} = -\omega^2\vec{u},\ \nabla\cdot\vec{u} = i\vec{k}\cdot\vec{u},\ \nabla\to i\vec{k}, \quad \text{(A.5)}$$

$$\Rightarrow \omega^2\vec{u} = c_s^2\vec{k}(\vec{k}\cdot\vec{u}) + i(\gamma-1)g\hat{z}(\vec{k}\cdot\vec{u}) + ig\vec{k}u_z. \quad \text{(A.6)}$$

To simplify more the equation and arrive to equation (52) we take the scalar product with $\vec{k}$

$$(\omega^2 - c_s^2k^2 - i(\gamma-1)gk_z)(\vec{k}\cdot\vec{u}) = igk^2u_z. \quad \text{(A.7)}$$

And the scalar product with $\hat{z}$

$$(c_s^2k_z + i(\gamma-1)g)(\vec{k}\cdot\vec{u}) = (\omega^2 - igk_z)u_z. \quad \text{(A.8)}$$

Now, dividing these equations we obtain

$$(\omega^2 - c_s^2k^2 - i(\gamma-1)gk_z)(\omega^2 - igk_z) = igk^2(c_s^2k_z + i(\gamma-1)g). \quad \text{(A.9)}$$

Rearranging the last equation we get

$$\omega^4 - i\gamma\omega^2gk_z - (\gamma-1)g^2k_z^2 - c_s^2k^2\omega^2 = -g^2k^2(\gamma-1) \quad \text{(A.10)}$$

$$\Rightarrow \omega^2(\omega^2 - i\gamma gk_z) = -g^2k^2(\gamma-1) + (\gamma-1)g^2k_z^2 + c_s^2k^2\omega^2. \quad \text{(A.11)}$$

And completing the square:

$$\omega^2\left(\omega^2 - \left(k_z + \frac{i\gamma g}{2}\right)^2 + k_z^2 - \frac{\gamma^2g^2}{4}\right) = -g^2k^2(\gamma-1) + (\gamma-1)g^2k_z^2 + c_s^2k^2\omega^2. \quad \text{(A.12)}$$

Introducing the terms: $\vec{k}' = \vec{k} + \frac{i}{2H}\hat{z} = \vec{k} + \frac{i\gamma g}{2}\hat{z}$, $k^2 = k'^2 + \frac{\gamma^2g^2}{4}$. We find

$$\omega^2\left(\omega^2 - k_z'^2 + k_z'^2 + \frac{\gamma^2g^2}{4} - \frac{\gamma^2g^2}{4}\right) = (\gamma-1)g^2\left(k_z'^2 + \frac{\gamma^2g^2}{4}\right) - (\gamma-1)g^2\left(k'^2 + \frac{\gamma^2g^2}{4}\right) + c_s^2\omega^2\left(k'^2 + \frac{\gamma^2g^2}{4}\right) \quad \text{(A.13)}$$

$$\Rightarrow \omega^2\left(\omega^2 - c_s^2\frac{\gamma^2g^2}{4}\right) = \left(\omega^2 - \frac{(\gamma-1)g^2}{c_s^2}\left(1 - \frac{k_z'^2}{k'^2}\right)\right)k'^2c_s^2. \quad \text{(A.14)}$$

To finally obtain the dispersion relation for acoustic-gravity waves (52):

$$\omega^2(\omega^2 - \omega_c^2) = (\omega^2 - N^2\sin^2\theta_g')k'^2c_s^2. \quad \text{(A.15)}$$

Where ω_c is the cut-off frequency, N^2 the Brunt Väisälä frequency and θ_g' is the angle between $\vec{k}'$ and the vertical ($\sin^2\theta_g' = 1 - \frac{k_z'^2}{k'^2}$).

Appendix B: Linearisation for MHD waves, dispersion relation

To found the system of linearised equations presented in section 4 (equations (68)-(72)) we have the following constants and perturbations for a homogeneous medium

$$\begin{cases} p = p_0 + p', \\ \rho = \rho_0 + \rho', \\ \vec{u} = \vec{u}', \\ \vec{B} = \vec{B_0} + \vec{B}'. \end{cases}$$

The continuity (68) and energy equation (69) are almost the same as the section 3, but without the gravity term. To linearise the energy equation we retain up to the first order terms.

$$\rho_0 \frac{\partial \vec{u}}{\partial t} = -\nabla(p' + p_0) + (\nabla \times (\vec{B}' + \vec{B_0})) \times \frac{(\vec{B}' + \vec{B_0})}{\mu_0} \tag{B.1}$$

$$\Rightarrow \rho_0 \frac{\partial \vec{u}}{\partial t} = -\nabla p' + (\nabla \times \vec{B}') \times \frac{\vec{B_0}}{\mu_0}. \tag{B.2}$$

Then, we do the same for the induction equation

$$\frac{\partial \vec{B}'}{\partial t} = \nabla \times (\vec{u} \times (\vec{B_0} + \vec{B}')) \tag{B.3}$$

$$\Rightarrow \frac{\partial \vec{B}'}{\partial t} = \nabla \times (\vec{u} \times \vec{B_0}). \tag{B.4}$$

Now, to calculate the wave equation we take the temporal derivative of equation (69):

$$\rho_0 \frac{\partial^2 \vec{u}}{\partial t^2} = -\frac{\partial}{\partial t}\nabla p' + \frac{\partial}{\partial t}(\nabla \times \vec{B}') \times \frac{\vec{B_0}}{\mu_0}. \tag{B.5}$$

We calculate the gradient of equation (70)

$$\frac{\partial}{\partial t}\nabla p' = -\gamma p_0 \nabla \cdot (\nabla \cdot \vec{u}). \tag{B.6}$$

And we take the rotational of equation (71)

$$\frac{\partial}{\partial t}(\nabla \times \vec{B}') = \nabla \times \left[\nabla \times (\vec{u} \times \vec{B_0})\right]. \tag{B.7}$$

Finally, replacing the terms in equations (B.6) and (B.7) in (B.5) we obtain the wave equation (73)

$$\frac{\partial^2 \vec{u}}{\partial t^2} = c_s^2 \nabla(\nabla \cdot \vec{u}) + \left[\nabla \times (\nabla \times (\vec{u} \times \vec{B_0}))\right] \times \frac{\vec{B_0}}{\mu_0 \rho_0}. \tag{B.8}$$

The solution given by equation (51) lead us to the dispersion relation (74)

$$\omega^2 \vec{u} = c_s^2 \vec{k}(\vec{k} \cdot \vec{u}) + \left[\vec{k} \times (\vec{k} \times (\vec{u} \times \vec{B_0}))\right] \times \frac{\vec{B_0}}{\mu_0 \rho_0}, \tag{B.9}$$

which can be simplified using vectorial identities like $(\vec{a}\times\vec{b})\times\vec{c}=\vec{b}(\vec{a}\cdot\vec{c})-\vec{a}(\vec{b}\cdot\vec{c})$:

$$\left[\vec{k}\times(\vec{k}\times(\vec{u}\times\vec{B}_0))\right]\times\frac{\vec{B}_0}{\mu_0\rho_0}= \tag{B.10}$$

$$(\vec{k}\times(\vec{u}\times\vec{B}_0))\left(\vec{k}\cdot\frac{\vec{B}_0}{\mu_0\rho_0}\right)-\vec{k}\left[((\vec{k}\times(\vec{u}\times\vec{B}_0))\cdot\frac{\vec{B}_0}{\mu_0\rho_0}\right]= \tag{B.11}$$

$$-\vec{B}_0(\vec{k}\cdot\vec{u})\left(\vec{k}\cdot\frac{\vec{B}_0}{\mu_0\rho_0}\right)+\vec{u}(\vec{k}\cdot\vec{B}_0)\left(\vec{k}\cdot\frac{\vec{B}_0}{\mu_0\rho_0}\right)+\vec{k}\left[(\vec{k}\cdot\vec{u})\vec{B}_0\cdot\frac{\vec{B}_0}{\mu_0\rho_0}-(\vec{k}\cdot\vec{B}_0)\vec{u}\cdot\frac{\vec{B}_0}{\mu_0\rho_0}\right]= \tag{B.12}$$

$$-\vec{B}_0(\vec{k}\cdot\vec{u})\left(\vec{k}\cdot\frac{\vec{B}_0}{\mu_0\rho_0}\right)+\frac{\vec{u}}{\mu_0\rho_0}(\vec{k}\cdot\vec{B}_0)^2+\vec{k}\frac{B_0^2}{\mu_0\rho_0}(\vec{k}\cdot\vec{u})-\vec{k}(\vec{k}\cdot\vec{B}_0)\frac{(\vec{B}_0\cdot\vec{u})}{\mu_0\rho_0}. \tag{B.13}$$

$$\Rightarrow\omega^2\vec{u}=c_s^2\vec{k}(\vec{k}\cdot\vec{u})-\frac{B_0k}{\mu_0\rho_0}\cos\alpha(\vec{k}\cdot\vec{u})\vec{B}_0+\frac{B_0^2k^2}{\mu_0\rho_0}\cos^2\alpha\vec{u}+\vec{k}\frac{B_0^2}{\mu_0\rho_0}(\vec{k}\cdot\vec{u})-\frac{B_0k}{\mu_0\rho_0}\cos\alpha\vec{k}(\vec{B}_0\cdot\vec{u}). \tag{B.14}$$

This is the general dispersion relation presented in section 4 when we take that the scalar product $\vec{k}\cdot\vec{B}_0=B_0k\cos\alpha$ where α is the *attack angle*.

Appendix C: Dispersion matrix and polarisation vectors

In order to obtain the dispersion relation in matrix form (88) presented in section 4.2.1 we start from equation (75) and by calculating their scalar products, the dispersion relation can be expressed in a matrix form:

$$\frac{\vec{u}}{\mu_0\rho_0}(\vec{k}\cdot\vec{B}_0)^2=\vec{u}v_A^2(k_x^2\sin^2\theta_m+2k_xk_z\sin\theta_m\cos\theta_m+k_z^2\cos^2\theta_m), \tag{C.1}$$

$$\vec{k}v_A^2(\vec{k}\cdot\vec{u})=\vec{k}v_A^2(k_xu_x+k_zu_z), \tag{C.2}$$

$$-\vec{B}_0(\vec{k}\cdot\vec{u})(\vec{k}\cdot\frac{\vec{B}_0}{\mu_0\rho_0})=-v_A^2(\sin\theta_m\hat{x}+\cos\theta_m\hat{z})(k_x^2u_x\sin\theta_m+k_xk_zu_x\cos\theta_m+k_xk_zu_z\sin\theta_m+k_z^2u_z\cos\theta_m), \tag{C.3}$$

$$-\vec{k}(\vec{k}\cdot\vec{B}_0)\frac{(\vec{B}_0\cdot\vec{u})}{\mu_0\rho_0}=-\vec{k}v_A^2(k_xu_x\sin^2\theta_m+k_xu_z\sin\theta_m\cos\theta_m+k_zu_x\sin\theta_m\cos\theta_m+k_zu_z\cos^2\theta_m). \tag{C.4}$$

Grouping into the vector components $\hat{x}$, $\hat{y}$, $\hat{z}$ and looking at the combinations of the velocities, gives the following dispersion matrix

$$\begin{pmatrix} c_s^2k_x^2+v_A^2k^2\cos^2\theta_m-\omega^2 & 0 & c_s^2k_xk_z-v_A^2k^2\cos\theta_m\sin\theta_m \\ 0 & v_A^2k_\parallel^2-\omega^2 & 0 \\ c_s^2k_xk_z-v_A^2k^2\cos\theta_m\sin\theta_m & 0 & c_s^2k_z^2-\omega^2+v_A^2k^2\sin^2\theta_m \end{pmatrix}\begin{pmatrix} ux \\ u_y \\ u_z \end{pmatrix}=0. \tag{C.5}$$

This dispersion matrix is block diagonal and one of its eigenvalues is the Alfvén waves relation, where $k_\parallel$ is the parallel component of $\vec{k}$ as shown in Figure 10. Alfvén's mode is decoupled from the fast and slow mode:

$$\lambda_A=\omega^2-v_A^2k_\parallel^2\Rightarrow\hat{y} \tag{C.6}$$

In section 4.2.1 we present directly the dispersion matrix (88) in the frame of reference where we suppress velocities in $\hat{y}$ direction, ignoring Alfvén waves. Then we diagonalise (88)

$$\begin{vmatrix} c_s^2k_x^2 + v_A^2k^2\cos^2\theta_m - \omega^2 - \lambda & c_s^2k_xk_z - v_A^2k^2\sin\theta_m\cos\theta_m \\ c_s^2k_xk_z - v_A^2k^2\cos\theta_m\sin\theta_m & c_s^2k_z^2 - \omega^2 + v_A^2k^2\sin^2\theta_m - \lambda \end{vmatrix} = 0, \tag{C.7}$$

$$(c_s^2k_x^2 - \omega^2 + v_A^2k^2\cos^2\theta_m - \lambda)(c_s^2k_z^2 - \omega^2 + v_A^2k^2\sin^2\theta_m - \lambda) - (c_s^2k_xk_z - v_A^2k^2\cos\theta\sin\theta_m)^2 = 0 \tag{C.8}$$

$$\Rightarrow -c_s^2\omega^2k^2 + c_s^2v_A^2k^2(k_x^2\sin^2\theta_m + k_z^2\cos^2\theta_m + 2c_s^2k_xk_zv_A^2k^2\cos\theta_m\sin\theta_m) - c_s^2k^2\lambda + \omega^4 - \omega^2v_A^2k^2 + +2\omega^2\lambda - v_A^2k^2\lambda + \lambda^2 = 0. \tag{C.9}$$

Introducing the relation of $\vec{k}$ to its parallel component $k_\parallel = k_x\sin\theta_m + k_z\cos\theta_m$ (Figure 10)

$$\lambda^2 + \lambda(2\omega^2 - c_s^2k^2 - v_A^2k^2) + \omega^4 - \omega^2(v_A^2k^2 + c_s^2k^2) + c_s^2v_A^2k^2k_\parallel^2 = 0 \tag{C.10}$$

$$\Rightarrow \lambda = \frac{-2\omega^2 + (c_s^2v_A^2)k^2}{2} \pm k^2\frac{\sqrt{(c_s^2+v_A^2)^2 - 4c_s^2v_A^2\cos^2\alpha}}{2}. \tag{C.11}$$

In order to arrive at the expression with $\cos\alpha$, the following relation was taken into account $\cos\alpha = \frac{k_\parallel}{k}$. Let us now turn to how the coefficients of the polarisation vectors at the two limits were derived in a little more detail than in the main text. Firstly, we derive the limit for the eigenvalues. The fast mode has for the $c_s \gg v_A$ limit that $\lambda_f \approx -\omega^2 + k^2c_s^2$ and for the $c_s \ll v_A$ $\lambda_f \approx -\omega^2 + k^2v_A^2$. For the slow mode in $c_s \gg v_A$ the eigenvalue:

$$\frac{\omega}{k} = \left[\frac{c_s^2+v_A^2}{2} - \frac{\sqrt{(c_s^2+v_A^2)^2 - 4c_s^2v_A^2\cos^2\alpha}}{2}\right]^{1/2} = \left[\frac{c_s^2}{2} - \frac{\sqrt{c_s^4 - 4c_s^2v_A^2\cos^2\alpha}}{2}\right]^{1/2} \tag{C.12}$$

$$\Rightarrow \left[\frac{c_s^2}{2} - \frac{c_s^2}{2}\left(1 - \frac{4v_A^2\cos^2\alpha}{c_s^2}\right)^{1/2}\right]^{1/2} \approx \left[\frac{c_s^2}{2} - \frac{c_s^2}{2}\left(1 - 2\frac{v_A^2\cos^2\alpha}{c_s^2}\right)\right]^{1/2} = v_A\cos\alpha. \tag{C.13}$$

For the approximation was used: $(1-x)^{1/2} \approx 1 - \frac{1}{2}x$ when $x \ll 1$. So, the eigenvalue $\lambda_s \approx -\omega^2 - k^2v_A^2\cos^2\alpha$. Then, in the $c_s \ll v_A$ limit

$$\frac{\omega}{k} = \left[\frac{v_A^2}{2} - \frac{\sqrt{v_A^4 - 4c_s^2v_A^2\cos^2\alpha}}{2}\right]^{1/2} = c_s\cos\alpha. \tag{C.14}$$

Where $\lambda_s \approx -\omega^2 - k^2c_s^2\cos^2\alpha$ is the approximation in this limit. Secondly, we are going to take the limits of the coefficients. Beginning with the fast mode, for $c_s \gg v_A$:

$$C_x^f = \frac{c_s^2k_xk_z - v_A^2k^2\cos\theta_m\sin\theta_m}{\sqrt{(c_s^2k_xk_z - v_A^2k^2\cos\theta_m\sin\theta_m)^2 + (\lambda_f - c_s^2k_x^2 + \omega^2 - v_A^2k^2\cos^2\theta_m)^2}} \approx \frac{c_s^2k_xk_z}{\sqrt{c_s^4k_x^2k_z^2 + (-\omega^2 + k^2c_s^2 - c_s^2k_x^2 + \omega^2)^2}} = \frac{c_s^2k_xk_z}{\sqrt{c_s^4k_x^2(k^2 - 2k^2 + \frac{k^4}{k_x^2})}} = \frac{k_z}{k\frac{k}{k_x}\sqrt{1 - \frac{k_x^2}{k^2}}} = \sin\phi. \tag{C.15}$$

Where ϕ is the angle that $\vec{k}$ forms with z axis (Figure 10). The second coefficient is

$$C_z^f = \frac{\lambda_f - c_s^2 k_x^2 + \omega^2 - v_A^2 k^2 \cos^2\theta_m}{\sqrt{(c_s^2 k_x k_z - v_A^2 k^2 \cos\theta_m \sin\theta_m)^2 + (\lambda_f - c_s^2 k_x^2 + \omega^2 - v_A^2 k^2 \cos^2\theta_m)^2}} \approx \frac{-\omega^2 + k^2 c_s^2 - c_s^2 k_x^2 + \omega^2}{c_s^2 k_x k \sqrt{\frac{k^2}{k_x^2} - 1}} = \frac{1}{\sqrt{1 - \frac{k_x^2}{k^2}}} - \frac{k_x}{k \frac{k}{k_x}\sqrt{1 - \frac{k_x^2}{k^2}}} = \frac{1}{\cos\phi} - \frac{\sin^2\phi}{\cos\phi} = \cos\phi. \tag{C.16}$$

The polarisation direction for fast waves when $c_s \gg v_A$ is parallel to the wave vector, since they are acoustic waves. This is explained in more detail in the main text. Moving on to the second limit $c_s \ll v_A$.

$$C_x^f = \frac{c_s^2 k_x k_z - v_A^2 k^2 \cos\theta_m \sin\theta_m}{\sqrt{(c_s^2 k_x k_z - v_A^2 k^2 \cos\theta_m \sin\theta_m)^2 + (\lambda_f - c_s^2 k_x^2 + \omega^2 - v_A^2 k^2 \cos^2\theta_m)^2}} \approx \frac{-v_A^2 k^2 \cos\theta_m \sin\theta_m}{\sqrt{v_A^4 k^4 \cos^2\theta_m \sin^2\theta_m + (-\omega^2 + k^2 v_A^2 + \omega^2 - v_A^2 k^2 \cos^2\theta_m)^2}} = \frac{-v_A^2 k^2 \cos\theta_m \sin\theta_m}{\sqrt{v_A^4 k^4 - v_A^4 k^4 \cos^2\theta_m}} = -\cos\theta, \tag{C.17}$$

$$C_z^f = \frac{\lambda_f - c_s^2 k_x^2 + \omega^2 - v_A^2 k^2 \cos^2\theta_m}{\sqrt{(c_s^2 k_x k_z - v_A^2 k^2 \cos\theta_m \sin\theta_m)^2 + (\lambda_f - c_s^2 k_x^2 + \omega^2 - v_A^2 k^2 \cos^2\theta_m)^2}} \approx \frac{-\omega^2 + k^2 v_A^2 + \omega^2 - v_A^2 k^2 \cos^2\theta_m}{\sqrt{v_A^4 k^4 - v_A^4 k^4 \cos^2\theta_m}} = \frac{1 - \cos^2\theta_m}{\sin\theta_m} = \sin\theta_m. \tag{C.18}$$

Now, they are polarised perpendicularly to the magnetic field, because they are magnetic waves. It is the turn of the slow mode when $c_s \gg v_A$

$$C_x^s = \frac{c_s^2 k_x k_z - v_A^2 k^2 \cos\theta_m \sin\theta_m}{\sqrt{(c_s^2 k_x k_z - v_A^2 k^2 \cos\theta_m \sin\theta_m)^2 + (\lambda_s - c_s^2 k_x^2 + \omega^2 - v_A^2 k^2 \cos^2\theta_m)^2}} \approx \frac{c_s^2 k_x k_z}{\sqrt{c_s^4 k_x^2 k_z^2 + (-\omega^2 - k^2 v_A^2 \cos^2\alpha - c_s^2 k_x^2 + \omega^2)}} = \frac{c_s^2 k_x k_z}{c_s^2 k_x k \sqrt{1 + 2\frac{v_A^2 \cos^2\alpha}{c_s^2}}} \approx \frac{k_z}{k} = \cos\phi, \tag{C.19}$$

$$C_z^s = \frac{\lambda_s - c_s^2 k_x^2 + \omega^2 - v_A^2 k^2 \cos^2\theta_m}{\sqrt{(c_s^2 k_x k_z - v_A^2 k^2 \cos\theta_m \sin\theta_m)^2 + (\lambda_s - c_s^2 k_x^2 + \omega^2 - v_A^2 k^2 \cos^2\theta_m)^2}} \approx \frac{-\omega^2 - k^2 v_A^2 \cos^2\alpha + \omega^2 - c_s^2 k_x^2}{\sqrt{c_s^4 k_x^2 k_z^2 + (-\omega^2 - k^2 v_A^2 \cos^2\alpha - c_s^2 k_x^2 + \omega^2)}} = \frac{-k^2 v_A^2 \cos^2\alpha}{k^2 v_A^2 \cos^2\alpha \sqrt{\frac{c_s^4 k_x^2}{k^4 v_A^4 \cos^4\alpha} + \frac{2 c_s^2 k_x^2}{v_A^2 k^2 \cos^2\alpha}}} - \frac{k_x}{k\sqrt{1 + 2\frac{v_A^2 \cos^2\alpha}{c_s^2}}} \approx -\sin\phi. \tag{C.20}$$

The slow mode is polarised in the perpendicular direction, since they are magnetic waves when $c_s \gg v_A$. Besides, as the fast and slow modes are eigenvalues their eigenvectors will be orthogonal to each other. When $c_s \ll v_A$

$$C_x^s = \frac{c_s^2 k_x k_z - v_A^2 k^2 \cos\theta_m \sin\theta_m}{\sqrt{(c_s^2 k_x k_z - v_A^2 k^2 \cos\theta_m \sin\theta_m)^2 + (\lambda_s - c_s^2 k_x^2 + \omega^2 - v_A^2 k^2 \cos^2\theta_m)^2}} \approx$$
$$\frac{-v_A^2 k^2 \cos\theta_m \sin\theta_m}{\sqrt{v_A^4 k^4 \cos^2\theta_m \sin^{\theta_m} + (-\omega^2 - k^2 c_s^2 \cos^2\alpha + \omega^2 - v_A^2 k^2 \cos^2\theta_m)^2}} =$$
$$\frac{-\sin\theta_m}{\sqrt{1 + 2\frac{c_s^2 \cos^2\alpha}{v_A^2}}} = -\sin\theta_m, \tag{C.21}$$

$$C_z^s = \frac{\lambda_s - c_s^2 k_x^2 + \omega^2 - v_A^2 k^2 \cos^2\theta_m}{\sqrt{(c_s^2 k_x k_z - v_A^2 k^2 \cos\theta_m \sin\theta_m)^2 + (\lambda_s - c_s^2 k_x^2 + \omega^2 - v_A^2 k^2 \cos^2\theta_m)^2}} \approx$$
$$-\frac{k^2 c_s^2 \cos^2\alpha}{k^2 c_s^2 \sqrt{\frac{v_A^4 \cos^2\theta_m}{c_s^4} + 2\frac{\cos^2\theta_m \cos^2\alpha v_A^2}{c_s^2}}} - \frac{\cos\theta_m}{\sqrt{1 + 2\frac{c_s^2\cos^2\alpha}{v_A^2}}} = -\cos\theta_m. \tag{C.22}$$

Finally, we have that the slow waves in the limit $c_s \ll v_A$ are parallel to the magnetic field, because they are acoustic waves and they are orthogonal to the fast one that are polarised perpendicularly, since they are magnetic waves in this limit.

Appendix D: Energy conservation

In order to find the energy equation in a conservative form (102), we take the scalar product with $\vec{u}$ in the momentum equation (69)

$$\frac{\partial}{\partial t}\left(\frac{1}{2}\rho_0 u^2\right) = -\nabla \cdot (p'\vec{u}) + p'\nabla \cdot \vec{u} - u_z \rho' g + \vec{u} \cdot \left[(\nabla \times \vec{B}') \times \frac{\vec{B}_0}{\mu_0}\right]. \tag{D.1}$$

Now, taking the scalar product $\vec{B}'/\mu_0$ with the induction equation (71)

$$\frac{1}{\mu_0}\frac{\partial}{\partial t}\left(\frac{1}{2}B'^2\right) = \frac{\vec{B}'}{\mu_0} \cdot \left[\nabla \times (\vec{u} \times \vec{B}_0)\right]. \tag{D.2}$$

To simplify the derivation, we can use the electric field perturbation as an auxiliary form:

$$\vec{E} = -\vec{u} \times \vec{B} \Rightarrow \vec{E}' = -\vec{u} \times \vec{B}_0, \tag{D.3}$$

where we use the ideal Ohm's law (5). Then replacing (D.3) in equation (D.2)

$$\frac{1}{\mu_0}\frac{\partial}{\partial t}\left(\frac{1}{2}B'^2\right) = -\frac{\vec{B}'}{\mu_0} \cdot (\nabla \times \vec{E}'). \tag{D.4}$$

Now, with the term $\vec{u} \cdot \left[(\nabla \times \vec{B}') \times \frac{\vec{B}_0}{\mu_0}\right]$ of equation (D.1) and using the properties of the mixed product:

$$\vec{a} \cdot (\vec{b} \times \vec{c}) = \begin{vmatrix} a_1 & a_2 & a_3 \\ b_1 & b_2 & b_3 \\ c_1 & c_2 & c_3 \end{vmatrix} = -\begin{vmatrix} b_1 & b_2 & b_3 \\ a_1 & a_2 & a_3 \\ c_1 & c_2 & c_3 \end{vmatrix} = -\vec{b} \cdot (\vec{a} \times \vec{c}), \tag{D.5}$$

$$\vec{u} \cdot \left[(\nabla \times \vec{B}') \times \frac{\vec{B}_0}{\mu_0}\right] = -(\nabla \times \vec{B}') \cdot \left(\frac{\vec{B}_0}{\mu_0} \times \vec{u}\right) = \frac{1}{\mu_0}\vec{E}' \cdot (\nabla \times \vec{B}'). \tag{D.6}$$

Using the vector identity $(\nabla \times \vec{A}) \cdot \vec{B} = \nabla \cdot (\vec{A} \times \vec{B}) + (\nabla \times \vec{B}) \cdot \vec{A}$ in equation (D.6)

$$\frac{1}{\mu_0}\vec{E} \cdot (\nabla \times \vec{B}') = \frac{1}{\mu_0}\left[\nabla \cdot (\vec{B}' \times \vec{E}') + (\nabla \times \vec{E}') \cdot \vec{B}'\right]. \tag{D.7}$$

Replacing the equation (D.4) we get

$$\frac{1}{\mu_0}\vec{E} \cdot (\nabla \times \vec{B}') = \frac{1}{\mu_0}\left[\nabla \cdot (\vec{B}' \times \vec{E}') - \frac{\partial}{\partial t}\left(\frac{1}{2}B'^2\right)\right] \tag{D.8}$$

$$\Rightarrow \frac{1}{\mu_0}\vec{E} \cdot (\nabla \times \vec{B}') = \frac{1}{\mu_0}\left[-\nabla \cdot (\vec{B}' \times (\vec{u} \times \vec{B}_0)) - \frac{\partial}{\partial t}\left(\frac{1}{2}B'^2\right)\right]. \tag{D.9}$$

And using the relation $\vec{c} \times (\vec{a} \times \vec{b}) = \vec{a}(\vec{b} \cdot \vec{c}) - \vec{b}(\vec{a} \cdot \vec{c})$,

$$\frac{1}{\mu_0}\vec{E} \cdot (\nabla \times \vec{B}') = -\frac{1}{\mu_0}\left[\nabla \cdot (\vec{u}(\vec{B}_0 \cdot \vec{B}')) - \nabla(\vec{B}_0(\vec{u} \cdot \vec{B}'))\right] - \frac{1}{\mu_0}\frac{\partial}{\partial t}\left(\frac{1}{2}B'^2\right). \tag{D.10}$$

Finally, replacing (D.10) in (D.1):

$$\frac{\partial}{\partial t}\left(\frac{1}{2}\rho_0 u^2\right) = -\nabla\cdot(p'\vec{u}) + p'\nabla\cdot\vec{u} - u_z\rho' g - \frac{1}{\mu_0}\left[\nabla \cdot (\vec{u}(\vec{B}_0 \cdot \vec{B}')) - \nabla(\vec{B}_0(\vec{u} \cdot \vec{B}'))\right] - \frac{1}{\mu_0}\frac{\partial}{\partial t}\left(\frac{1}{2}B'^2\right). \tag{D.11}$$

We have already dealt with the magnetic terms and it remains to manipulate the other terms, which we have developed previously in section 3.3.1. Therefore, if we derivate the other terms like in subsection 3.3.1 from (D.11) we obtain the conservation equation (102).

References

Abramowitz, M., Stegun, I. A., & Romer, R. H. 1988, Handbook of mathematical functions with formulas, graphs, and mathematical tables, American Association of Physics Teachers

Bhatnagar, A., & Livingston, W. C. 2005, Fundamentals of solar astronomy, Vol. 6 (World Scientific)

Biermann, L. 1946, Naturwissenschaften, 33, 118

Bittencourt, J. A. 2004, Fundamentals of plasma physics (Springer Science & Business Media)

Boyd, T. M., Boyd, T., & Sanderson, J. 2003, The physics of plasmas (Cambridge university press)

Bray, R., & Loughhead, R. 1974, The Solar Chromosphere, International astrophysics series (Chapman and Hall [distributed by Halsted Press, New York)

Cally, P. S., & Gómez-Míguez, M. M. 2023, The Astrophysical Journal, 946, 108, doi: 10.3847/1538-4357/acbb63

Christensen-Dalsgaard, J. 2002, Reviews of Modern Physics, 74, 1073

Clarke, C., & Carswell, B. 2007, Principles of astrophysical fluid dynamics (Cambridge University Press)

Eckart, C. 2013, Hydrodynamics of oceans and atmospheres (Elsevier)

Goedbloed, J. P., & Poedts, S. 2004, Principles of magnetohydrodynamics: with applications to laboratory and astrophysical plasmas (Cambridge university press)

Goossens, M. 2003, An introduction to plasma astrophysics and magnetohydrodynamics, Vol. 294 (Springer Science & Business Media)

Landau, L. D., & Lifshitz, E. M. 2013, Fluid Mechanics: Landau and Lifshitz: Course of Theoretical Physics, Volume 6, Vol. 6 (Elsevier)

Lighthill, J. 2001, Waves in fluids (Cambridge university press)

NASA/SDO. 2023, NASA's Solar Dynamics Observatory. https://www.nasa.gov/mission_pages/sdo/how-sdo-sees-the-sun

Priest, E. 2014, Magnetohydrodynamics of the Sun (Cambridge University Press)

Schunker, H., & Cally, P. 2006, Monthly Notices of the Royal Astronomical Society, 372, 551 , doi: 10.1111/j.1365-2966.2006.10855.x

Schwarzschild, M. 1948, The Astrophysical Journal, 107, 1

Stix, M. 2004, The sun: an introduction (Springer Science & Business Media)

Tracy, E. R., Brizard, A. J., Richardson, A. S., & Kaufman, A. N. 2014, Ray Tracing and Beyond: Phase Space Methods in Plasma Wave Theory (Cambridge University Press), doi: 10.1017/CBO9780511667565